JAERI-Research
95-057

PRESENT STATUS OF R&D ON HYDROGEN PRODUCTION BY HIGH TEMPERATURE ELECTROLYSIS OF STEAM

August 1995

Ryutaro HINO, Hideki AITA, Kenji SEKITA
Katsuhiro HAGA, Yoshiaki MIYAMOTO and Tomo-o IWATA*

日本原子力研究所
Japan Atomic Energy Research Institute

本レポートは，日本原子力研究所が不定期に公刊している研究報告書です。

入手の問合わせは，日本原子力研究所技術情報部情報資料課（〒319-11 茨城県那珂郡東海村）あて，お申し越しください。なお，このほかに財団法人原子力弘済会資料センター（〒319-11 茨城県那珂郡東海村日本原子力研究所内）で複写による実費頒布をおこなっております。

This report is issued irregularly.

Inquiries about availability of the reports should be addressed to Information Division, Department of Technical Information, Japan Atomic Energy Research Institute, Tokai-mura, Naka-gun, Ibaraki-ken 319-11, Japan.

編集兼発行　日本原子力研究所

印　　刷　㈱原子力資料サービス

Present Status of R&D on Hydrogen Production by High Temperature Electrolysis of Steam

Ryutaro HINO, Hideki AITA, Kenji SEKITA
Katsuhiro HAGA, Yoshiaki MIYAMOTO and Tomo-o IWATA*

Department of High Temperature Engineering
Tokai Research Establishment
Japan Atomic Energy Research Institute
Tokai-mura, Naka-gun, Ibaraki-ken

(Received July 28, 1995)

In JAERI, design and R&D works on hydrogen production process have been conducted for connecting to the HTTR under construction at the Oarai Establishment of the JAERI as the nuclear heat utilization system. As for a hydrogen production process by high-temperature electrolysis of steam, laboratory-scale experiments have been conducted using a practical electrolysis tube with 12 cells connected in series. Hydrogen was produced at a maximum density of 44 Nml/ cm^2h at 950℃, and know-how of operational procedures and operational experience have been also accumulated. Then, a self-supporting planar electrolysis cell was fabricated in order to improve hydrogen production performance. In the preliminary test with the planar cell, hydrogen has been produced continuously at a maximum density of 36 Nml/cm^2h at lower electrolysis temperature of 850℃.

This report presents typical test results mentioned above, a review of previous studies conducted in the world and R&D items required for connecting to the HTTR.

Keywords: Hydrogen Production, HTTR, Nuclear Heat Utilization, High-temperature Electrolysis, Steam, Laboratory-scale Experiment, Electrolysis Tube, Planar Cell, Review

---

* Fuji Electric Corporate Research and Development, Ltd.

高温水蒸気電解による水素製造法の研究開発の現状

日本原子力研究所東海研究所高温工学部
日野竜太郎・会田　秀樹・関田　健司・羽賀　勝洋
宮本　喜晟・岩田　友夫*

（1995年7月28日受理）

原研で建設中のＨＴＴＲに接続することを目的とした水素製造プロセスの設計検討及び研究開発を進めている。このうち高温水蒸気電解による水素製造法について，これまでに実用的な12セル構造の円筒型電解要素を用いて実験室規模の試験を行い，950℃において単位電解面積当たり約44Nml/㎠hの速度で水素を発生させることに成功するとともに，電解試験手順などのノウハウと運転経験を蓄積した。その後，水素製造能力の向上を目指し，電解質自立方式の平板型電解要素を試作し，予備試験では850℃という低温域において約36Nml/㎠hの速度で水素を連続的に発生させることができた。

本報告では，上記試験の代表的な結果のほか，他機関で実施された高温水蒸気電解試験結果及びＨＴＴＲ接続のために必要なＲ＆Ｄについて述べる。

東海研究所：〒319-11　茨城県那珂郡東海村白方白根2-4
＊㈱富士電機総合研究所

Contents

目　　次

1. Introduction

Nuclear heat generated by LWR has already used to commercial power generation. If nuclear heat is applied to the nonelectric field such as chemical and steel industries, nuclear energy will contribute to greatly reduce an amount of CO_2 discharged to the atmosphere. High-temperature gas-cooled reactors (HTGRs) have high potential for application to nonelectric fields as well as the electric power generation as high-temperature heat sources up to 1000℃.

The High-Temperature Engineering Test Reactor (HTTR), the first HTGR in Japan, is now constructing at the site of the Oarai Research Establishment of Japan Atomic Energy Research Institute (JAERI). One of the key objectives of the HTTR is to demonstrate effectiveness of high-temperature nuclear heat utilization. The first heat utilization system is planned to be connected to the HTTR in about five years after the first criticality of the HTTR to be achieved in 1998. Of the HTTR thermal output of 30MW, 10MW is transferred to the heat utilization system through a helium-to-helium intermediate heat exchanger.

The following design and/or R&D works focused on hydrogen production have been carried out in JAERI:

1) Design and experimental works for hydrogen and methanol coproduction system: steam/methane reforming process coupled with methanol synthesis process,
2) Laboratory-scale experiments for a thermochemical water splitting by Iodine-Sulfur (IS) process,
3) Laboratory-scale experiments for a high-temperature electrolysis of steam using ceramic electrolysis cells.

As for hydrogen production, almost the total hydrogen demand is presently met by hydrogen made from fossil fuels, by steam reforming and partial oxidation of natural gas or oil fractions, although hydrogen could be simply produced from water by electrolysis. Electrolysis of water to provide hydrogen for chemical processes plays only a minor role today because its hydrogen production cost is much higher than that from fossil fuels; less than 1% of worldwide hydrogen demand is produced electrolytically.

In the water electrolysis, there is no commercial large scale units except the conventional alkaline electrolysis unit which have rather low current efficiency of 80% or less. Many advanced concepts of electrolytic hydrogen production have been proposed to improve hydrogen production efficiency and to reach high hydrogen production density from the viewpoint of saving electricity. A water electrolysis using solid

polymer membranes (solid polymer electrolysis, SPE) and the high-temperature electrolysis of steam (HTES) using ceramic electrolysis cells are representative of new advanced technologies. Current efficiency of the SPE is of the order of 85-90% in the laboratory-scale and prototype experiments, and that of the HTES is around 100% in the laboratory-scale experiments.

Figure 1.1 shows an energy demand for water and steam electrolysis. Total energy demand ($\triangle H$) for water and steam decomposition is the sum of the Gibbs energy ($\triangle G$) and the heat energy ($T\triangle S$). The electrical energy demand, $\triangle G$, decreases with increasing temperature as shown in the figure; the ratio of $\triangle G$ to $\triangle H$ is about 93% at 100℃ and about 70% at 1000℃. On the other hand, higher temperature favor electrode reaction and helps in lowering cathodic and anodic overvoltages: it is possible to increase current density at higher temperature. Thus, the HTES is favored from both thermodynamic and kinetic standpoints. Lower cell voltage and higher current density are simultaneously achievable in high-temperature operation. Furthermore, there is almost no corrosion problem on the ceramic electrolyte of the electrolysis cell.

The HTES, however, is at a very early stage of technology, and thus, significant development effort is required to solve severe materials and fabrication problems due to high-temperature operation. We are now conducting laboratory-scale experiments to improve and upgrade the HTES technology. This report presents a reaction scheme, our typical test results and future works as well as an outline of the state-of-the-art of electrolysis cell fabrication and HTES test results obtained using practical electrolysis cells in the past.

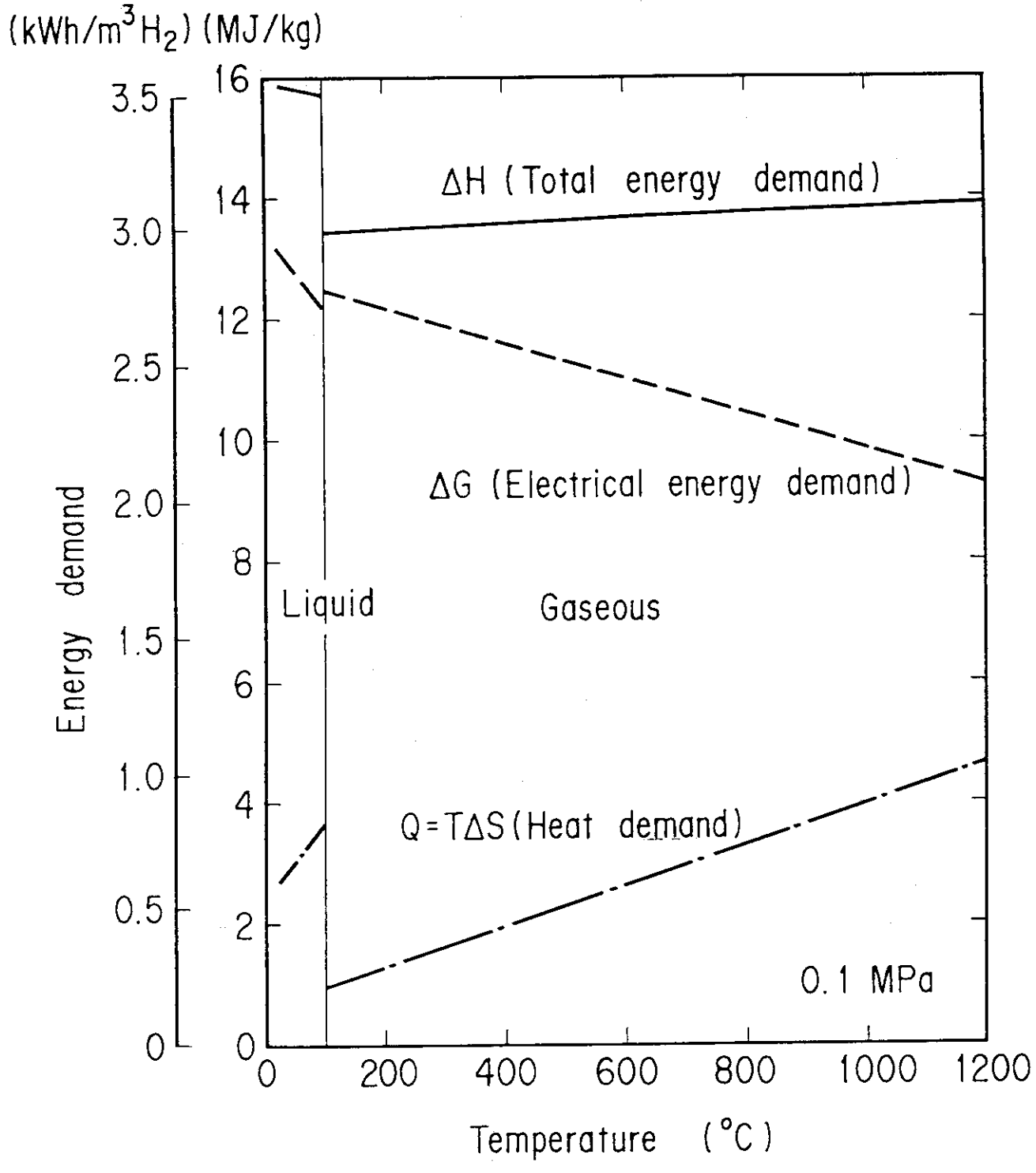

Fig. 1.1 Energy demand for water and steam electrolysis

2. Reaction Scheme in High-Temperature Electrolysis of Steam

The process of the high-temperature electrolysis of steam (HTES) is a reaction reverse to a solid-oxide fuel cell (SOFC) developing vigorously in the world: an oxygen ionic conductor is mainly used as a solid-oxide electrolyte as shown in **Fig. 2.1**. An electrolysis cell consists of the electrolyte, a cathode (negative electrode) and an anode (positive electrode): electrodes are good electron conductors. Steam at the cathode is dissociated with electrons from externally provided electricity on the cathode surface: a potential in excess of the Gibbs energy value is applied. Hydrogen molecules form on the cathode surface: $H_20(g) + 2e^- \rightarrow H_2(g) + O^{2-}$. Simultaneously oxygen ions migrate through oxygen vacancies in the lattice of the electrolyte material, a mixed oxide such as ZrO_2/Y_2O_3, and oxygen molecules forms on the anode surface with the release of electrons: $O^{2-} \rightarrow 1/2O_2(g) + 2e^-$. Reactions on the two electrodes are summed to as follows:

$$H_2O(g) \rightarrow H_2(g) + 1/2O_2(g) \qquad (2.1)$$

The products, hydrogen and oxygen, are separated by the gastight electrolyte. Thus, the process produces high purity hydrogen.

Konishi et al. indicated a relation between a hydrogen production rate and an applied voltage to the cell on the basis of the Nernst equation [1]. Then, the Gibbs free energy change, $\triangle G$, for the reaction (2.1) is

$$\triangle G = \triangle G_o + RT \ln (a_{H2}\, a_{O2}^{1/2} / a_{H2O}) \qquad (2.2)$$

where $\triangle G_o$ is the standard Gibbs free energy change (per mole) for the reaction (2.1) at a temperature of T, R is the gas constant, and a_{H2}, a_{O2} and a_{H2O} are the activities of H_2, O_2 and H_2O in the cell. This relation can also be written using relations of $E=\triangle G/2F$ and $E_o=\triangle G_o/2F$

$$E = E_o + (RT/2F) \ln(a_{H2}\, a_{O2}^{1/2} / a_{H2O}) \qquad (2.3)$$

where F is Faraday constant. This equation is equivalent to the Nernst equation for the electromotive force (e.m.f.) of the fuel cell using H_2 and O_2, where E_o ($=\triangle G_o/2F$) is the standard e.m.f. of following reaction in the quasi-static state: $H_2(g) + 1/2O_2(g) \rightarrow H_2O(g)$. For an electric power required for the electrolysis, following relation are given:

$$\triangle G = 2F \times E = 2.393 \times E \qquad [Wh/Ndm^3] \qquad (2.4)$$

Activities of reactants and products are expressed as partial pressures in the cell because the reaction proceeds in the gas phase regardless of the electrolyte. On the

other hand, applied voltage shall increase with polarization in operating the cell. Increment of voltage, η, is called an overvoltage, which consists of an activation overvoltage by electrode reaction, a concentration overvoltage by disturbance of steam supply at the cathode and a resistance overvoltage by electrical resistance including electrical leads, interconnections and others. Then equation (2.3) is rewritten as follows:

$$E = E_o + (RT/2F) \ln(P_{H2} P_{O2}^{1/2} / P_{H2O}) + \eta \qquad (2.5)$$

where P_{H2} and P_{H2O} are the partial pressures of H_2 and H_2O at the cathode, respectively, and P_{O2} the partial pressure of O_2 at the anode.

In the model cell shown in Fig. 2.1, steam of molar flow rate f_o and pressure P_o is reduced to hydrogen gas of flow rate $f_o - f$ and partial pressure $P_o(f_o - f)/f_o$ in the cathode compartment: $(f_o - f)/f_o$ is a conversion rate from steam to hydrogen (steam conversion rate). The partial pressure of oxygen at the anode, P_{O2}, is assumed to be unity: the number of molecules does not change in the reaction at the cathode. Gaseous reactants and products are assumed to be mixed well so that almost all the molecules are carried to the reaction point on the cathode surface. In this condition, the gases in the cell are related to the applied voltage on the cathode, and the composition of the gas at the outlet of the cell in the steady state is expressed by equation (2.5). Using the molar flow rates, equation (2.5) can be written as follows:

$$E - \eta = E_o + (RT/2F) \ln \{(f_o - f)/f\} \qquad (2.6)$$

In terms of currents, $I=2F(f_o - f)$ and $I_o=2Ff_o$, equation (2.6) can also be written

$$E - \eta = E_o + (RT/2F) \ln \{I/(I_o - I)\} \qquad (2.7)$$

and using the steam conversion rate, $x=(f_o - f)/f_o$, equation (2.6) can also be written

$$E - \eta = E_o + (RT/2F) \ln \{x/(1 - x)\} \qquad (2.8)$$

The values of $E - \eta$ are the open circuit voltage or the IR-free voltage of the cell which is related to the composition of the product. It should be noted that the steam conversion rate x depends on the IR-free voltage and is not affected by the pressure or flow rate of the reactant. **Figure 2.2** shows the results calculated from eq.(2.8). As seen in the figure, the steam conversion rate rises to 99.9% at about 1.3V of the IR-free voltage and approaches to unity at higher voltage. The values of E_o at each temperature corresponds to the points of x=0.5. Because of the endothermic nature of the reaction, the IR-free voltage decreases with increasing temperature. Due to the temperature dependence of the logarithmic term in eq.(2.9), however, this effect decreases with the value of x.

In the electrolysis, various kinds of cell efficiencies are evaluated using applied voltage E, applied current I, and hydrogen production rate Q [Ndm^3/h] evaluated at 0.1MPa (1atm) and 273K (0℃), and so forth: electrolysis efficiencies for the practical electrolysis units had better be evaluated on the basis of the applied power.

Faraday efficiency ε_f is a ratio of the Gibbs free energy change $\triangle G$ and the applied power, $I \times E$: $\triangle G$ is related to the IR-free voltage. Then, Faraday efficiency is

$$\varepsilon_f = \triangle G / (I \times E)$$
$$= 2.393 \times (E - \eta) \times Q / (I \times E) \quad (2.9)$$

On the other hand, energy efficiency ε_e is a ratio of combustion heat of hydrogen $\triangle H$ along the reaction ($H_2(g) + 1/2O_2(g) \rightarrow H_2O(g)$) and applied power, which is defined as follows:

$$\varepsilon_e = \triangle H \times Q / 22.4 / (I \times E) \quad (2.10)$$

where $Q/22.4$ [Ndm^3/h] is a mole number of produced hydrogen. The lower heating value (L.H.V.) without the latent heat of water is used as the enthalpy of formation in above equation. The value of $\triangle H$ [kJ/mol] at temperature of T[K] is given as follows:

$$\triangle H = \triangle H_o + \int_{298}^{T} Cp dT$$

$$= \triangle H_o + \int_{298}^{T} \{(-11.8 + 4.9 \times 10^{-3} \times T + 0.35 \times 10^{-5} \times T^{-2})/1000\}\, dT$$

$$\cdots\cdots\cdots\cdots\cdots\cdots\cdots\cdots (2.11)$$

where $\triangle H_o$ is the lower heating value of hydrogen (L.H.V.) at 298K (25℃), -241.8 kJ/mol.

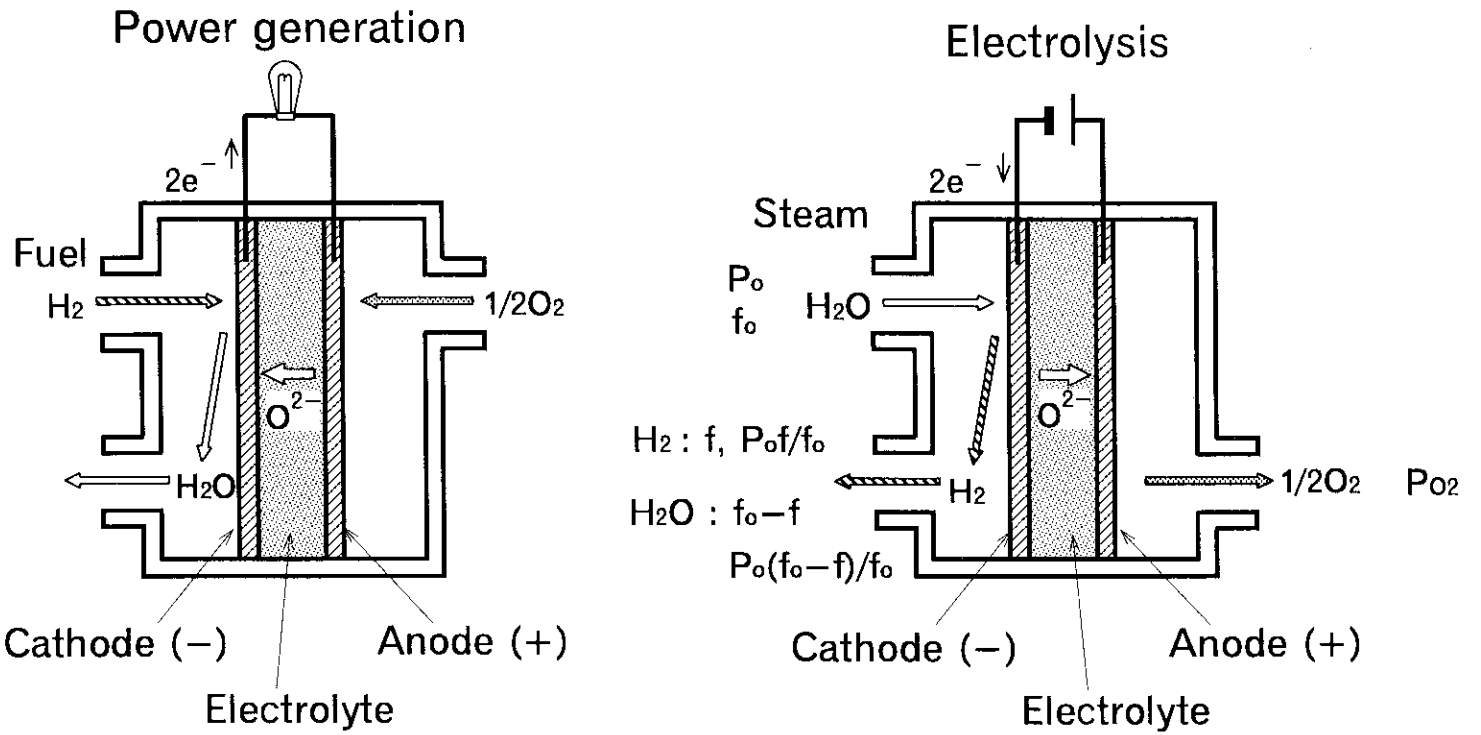

Cathodic reaction	$H_2+O^{2-} \rightarrow H_2O+2e^-$	$H_2O+2e^- \rightarrow H_2+O^{2-}$
Anodic reaction	$1/2O_2+2e^- \rightarrow O^{2-}$	$O^{2-} \rightarrow 2e^-+1/2O_2$
Total reaction	$H_2+1/2O_2 \rightarrow H_2O$	$H_2O \rightarrow H_2+1/2O_2$

Fig. 2.1 Principle of high-temperature electrolysis of steam
(Reverse reaction of solid oxide fuel cell)

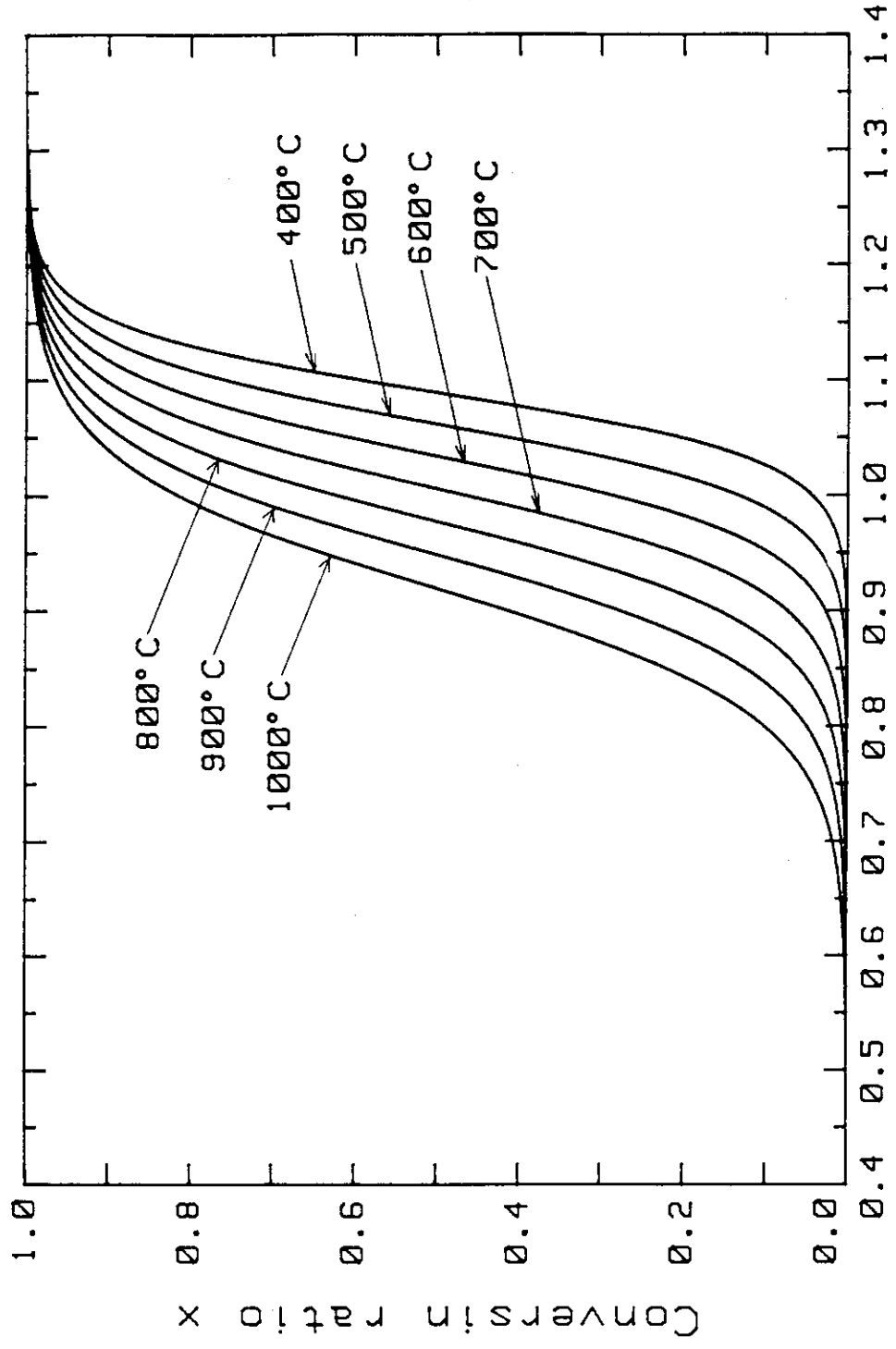

Fig. 2.2 Relationship between IR-free voltage and steam conversion rate

3. R&D Status of High-Temperature Electrolysis of Steam

Fabrication of the electrolysis cell is one of key technologies on the HTES. The electrolysis cell has the same structure as the SOFC. Almost all of materials composed of the SOFC are ceramics, and thus the SOFC is called a ceramic fuel cell. Several types of ceramic fuel cell structures have been proposed and fabricated. In this chapter, we will outline features of representative cell structures and show typical test results of the HTES using practical cells except ours.

3.1 Cell structure

At present, three common cell structures have been proposed and fabricated for the SOFC: tubular, planar and monolithic cell structures. Tubular and planar cell structures are popular in the SOFC and have been used in the laboratory-scale experiments of the HTES; but the monolithic cell structure is an advanced one at a very early stage of development.

We will outline features of tubular and planar cell structures on the basis of reviews [2,3]. In this section, the anode is defined as the positive electrode, and the cathode as the negative electrode.

(1) Single-cell tube

There are two types of the tubular structure: a single-cell and multicell tubes. The single-cell tube has been developed by Westinghouse Electric Co. **Figure 3.1** shows the single-cell tube called a Westinghouse tubular cell. The cell components are formed as thin layers on a closed-one-end tubular support. The present support tube is a porous 15mol%-calcia-stabilized ZrO_2 tube with porosity of around 35%, which has an inside diameter of 12 to 13mm, a wall thickness of 1 to 1.5mm and maximum length of 1000mm. The support tube is overlaid with a 1.4mm porous strontium-doped $LaMnO_3$ as the anode (positive electrode). A gastight Y_2O_3-stabilized ZrO_2 (YSZ) containing 10mol% of Y_2O_3 electrolyte layer covers the anode except in a strip of about 9mm along the cell active length with a thickness of 40 μ m. This strip of exposed anode is covered with a 40 μ m gastight magnesium-doped $LaCrO_3$ interconnection layer. The 100 μ m nickel ／stabilized ZrO_2 cermet (Ni cermet) cathode (negative electrode) covers the entire electrolyte surface.

The Westinghouse tubular cell is fabricated by a following manufacturing process.

(i) The support tube is fabricated by extrusion of a plastic mixture of calcia-stabilized ZrO_2 (CSZ) powder plus cellulose and starch as pore forms, followed by sintering in air at about 1550℃: the extrusion process is the preferred low-cost method of forming large quantities of support tube.

(ii) The anode is fabricated by depositing a slurry of doped $LaMnO_3$ on the support tube and sintering in air at about 1400℃. The interconnection is made by the EVD (Electrochemical Vapor Deposition) technique. Then masking is used to limit the deposition of interconnection into the narrow strip along the length of the cathode.

(iii) The electrolyte is also made by the EVD. The electrolyte is deposited over the entire active area of the cell, including overlap regions of about 0.5mm on all side of the interconnection.

(iv) The cathode is applied by dipping the cell in a nickel slurry. The anode covers the entire electrolyte surface, but not in contact with the interconnection, to avoid internal cell shorting. The anode is then fixed by the EVD of doped ZrO_2 in the nickel matrix. This ZrO_2 acts as a sintering inhibitor and maintains the porous and structurally stable anode.

The EVD process is the key fabrication technique in the Westinghouse tubular cell. The principle is shown in Minh's review [3]. The Westinghouse tubular cell has been fabricated in a number of different sizes; they have exhibited stable performance. Modules stacked cells have also constructed and demonstrated, which have different power output. For example, the module containing 576 cells has been operated at the output power of around 16.5kW for about 4,300h at Rokko New Energy Research Center in Japan [4].

(2) Multicell tube

The multicell tube has two types of structure as shown in **Fig. 3.2**: a banded-cell and a self-supporting tubes. In these tubes, segmented cells are connected in electrical and gas flow series. The interconnection provides sealing and electrical contact between the anode of one cell and the cathode of the next cell.

The banded-cell tube is supported by a ZrO_2 or a CSZ tube. Cell components of electrolyte, electrodes and others are layered on the support tube: each layer thickness is 100 to 300 μ m. For the self-supporting tube, individual cells form into short cylinders of about 15mm in diameter and 0.3 to 1mm in thickness to provide a structural support. In these multicell arrangement, the cell length is kept short to minimize the current path in

the electrodes so as to realize uniform current density. The multicell tube are fabricated as follows:

(i) Banded-cell tube

The support tube is formed by the almost same method as that the single-cell tube, which has a porosity of 34 to 38%, the outside diameter of around 21mm, the wall thickness of 2 to 3mm, and the length of around 710mm. Gastight Al_2O_3 layers are first applied on the support tube by a plasma spraying. The function of thin Al_2O_3 layers is to provide sealing at interconnecting areas. Thin copper tapes are used for masking to make the required pattern on the support tube. During spraying, the support tube rotates around its axis while the spray gun traverses along the support tube length. The porous cathode of Ni cermet is coated on the support tube by an acetylene flame spraying with thickness of 80 to 110 μ m. Then, the electrolyte of Y_2O_3-stabilized (8mol%) ZrO_2 is plasma sprayed on the cathode after masking: 100 to 150 μ m in thickness. The electrolyte layer is required to achieve gastightness without pinholes. The gastightness of the electrolyte has been improved by applying a low-pressure plasma spraying [5]. Recently, a coating technique based on a CO_2 laser has been developed for making electrolyte layers at the Electrotechnical Laboratory in Japan.

The interconnection, NiAl layer of less than 250 μ m in thickness, is fabricated by the plasma spraying. The interconnection at the both ends of the support tube works as electric leads and is covered with an Al_2O_3 coating of about 100 μ m thick to prevent oxidation during cell operation. The anode is deposited on the electrolyte and interconnection layers up to 200 μ m thick by the acetylene flame spraying. Calcium- or strontium- doped $LaCoO_3$ or strontium-doped $LaMnO_3$ is usually used for the anode.

At present, development works on the multicell tube are focused on improving assembling techniques of the banded-cell tubes in order to fabricate the module as module as well as increasing the durability of the tubes. The banded-cell tubes with 12 and 15 cells have been fabricated, and furthermore, a 1kW module containing 48 tubes with 12 cells have been constructed and operated for 1,000h continuously [6]. As for increasing the durability of the tube, a new type support tube made of porous metallic tube is now developing [7].

(ii) Self-supporting tube

The self-supporting tube have been developed at Dornier System GmbH in Germany [8]. The self-supporting tube was fabricated as follows [9].

1) Tubular structure was formed to connect electrolysis cylinders with interconnection rings in series by a diffusion welding to provide electric path and to keep gastightness.

2) Electrodes were prepared inside and outside of the tube structure by the spraying technique using a suitable masking procedure.

3) The tubular structure coated electrodes was sintered in high- temperature conditions to complete the electrolysis tube.

The gastight electrolyte cylinder is made of YSZ of 0.3mm thick. The electrodes are $LaMnO_3$ for the anode and Ni cermet for the cathode: thickness of each electrode is up to 500 μ m. Active dimensions of the segmented cells are around 10mm in length and 14mm in diameter.

Dornier System GmbH fabricated a module containing 10 ten-cell tubes and used it to the HTES experiments.

(3) Planar cell

There are two types of the planar cell configuration as shown in **Fig. 3.3**: a self-supporting and a substrate-supporting cells. The self-supporting cell supported by an electrolyte plate is a popular configuration; its fabrication cost is estimated at the lowest among other SOFC structures because of the simplest fabrication [10]. The electrodes are coated on the electrolyte YSZ plate by the slurry coating, a screen printing, or a tape casting. Porous Ni cermet is used for the cathode and strontium-doped $LaMnO_3$ for the cathode: each electrode thickness is more than 30 μ m. A 1kW module containing 94 cells has been demonstrated with a power density of 0.14 W/cm^2: each cell has an $100cm^2$ active electrode area [11].

As for the substrate-supporting cell, the substrate made of anode materials such as $LaMnO_3$ is generally used. This type cell has better abilities than the self-supporting cell: it is possible to enlarge an active area and to make thinner the electrolyte to reduce electrical resistance so as to increase cell power density. The electrolyte and the cathode is coated on the substrate of the anode by the plasma-spraying. Materials of the cathode, the anode and the electrolyte are the almost same as those of the tubular cell described above. The substrate has the thickness of 2 to 3mm, and thickness of coated layers of the anode and the electrolyte is less than 150 μ m. The cell active area of $200cm^2$ has been fabricated and is being improved the substrate to enlarge cell size to $300cm^2$ [12].

Internal resistance losses of the planar cell are independent of cell area because of in-plane electrical conduction, so that the planar cell offers improved power density in comparison with the tubular multicell structure.

The planar cell, however, requires high-temperature seals at the edges of the electrolyte plates or the substrata. High-temperature seal is especially important in fabricating the module stacked number of cells. Compressive seals, cement seals, glass seals and glass- ceramic seals have been proposed. The compressive seal - a simpler seal - can lead to a nonuniform stress distribution on the plate and thus, is liable to make cracks in the cell. Cements and glasses tend to react with cell materials at 1000℃ operating temperature.

3.2 Typical test results obtained in the past

In this section, we will show typical test results which have obtained with practical electrolysis cells until now in the world. Our test results are shown in the next chapter.

(1) Germany

In Germany, the HTES development had been performed by Dornier- system GmbH and Lurgi GmbH in cooperation with Robert Bosch GmbH since the middle of 70's, which had been sponsored by the German Government, in order to demonstrate the HTES process using a pilot plant; the demonstration test program including R&D on cell components and module technologies is called the HOTELLY (High Operating Temperature Electrolysis) program. The HOTELLY program focused on the HTES initially has included investigation of the SOFC application since 1987. Experimental results on the HTES have not been reported recently.

Cells and electrolysis modules had been practically developed by Dornier-system GmbH. Dornier-system GmbH had fabricated self-supporting electrolysis tubes connected up to 20 cells in series and had accumulated extensive experiences on operation of the HTES using 10-cell electrolysis tubes. Cell specifications were as follows [8,9,13];

Active cell length	:	10mm
Active cell diameter	:	14mm
Thickness of electrolyte	:	0.3mm
Thickness of anode	:	less than 0.25mm

Thickness of cathode	:	less than 0.1mm
Electrolyte	:	YSZ (Y_2O_3 containment 8 to 12mol%)
Cathode	:	Ni cermet
Anode	:	$LaMnO_3$ (probably)
Interconnection	:	dimensions and material are not clear.

Typical hydrogen production test with the 10-cell electrolysis tube was conducted under following conditions [13]:

Electrolysis temperature	:	997℃
Pressure	:	near atmospheric pressure
Inlet gas flow rate	:	17 Nml/min (H_2)／136 Nml/min (H_2O) (at standard conditions of 1atm and 0℃)
Applied voltage	:	max. 13.3 V
Current density	:	max. 0.37 A/cm^2

Under this condition, an outlet hydrogen content increased to 85%. From this test results, maximum DC current, electrical resistance, hydrogen production rate and others were calculated as follows:

max. DC current $0.37[A/cm^2] \times (1.4[cm] \times \pi \times 1[cm]$: active cell area)
$= 1.63$ [A]

max. applied power $1.63[A] \times 13.3[V] = 21.7$ [W]

max. electrical resistance $13.3[V] / 1.63[A] = 8.2$ [Ω]

Hydrogen production rate (α)

$(17[Nml/min(H_2)] + \alpha) / \{(136[Nml/min(H_2O)] - \alpha) + (\alpha + 17[Nml/min(H_2)]\}$
$= 0.85$
$\alpha = 113$ [Nml/min] $= 6.78$ [Ndm^3/h (H_2)]

Hydrogen production density of a cell

$6780[Nml/h(H_2)] \times (1.4[cm] \times \pi \times 1[cm] \times 10cells)$
$= 154$ [Nml/cm^{2}h (H_2)]

Hydrogen production rate per applied power

$6780[Nml/h(H_2)] / 21.7[W]$
$= 312$ [Nml/W (H_2)]

Conversion rate from steam to hydrogen (stem conversion rate)

$$113[\mathrm{Nml/min\ (H_2)}] \ / 136[\mathrm{Nml/min\ (H_2O)}]$$
$$= 0.83$$

In the case where the HTES plant is added onto an existing electric power plant, steam conversion rate more than 50% is preferable in order to keep overall thermal efficiency [14]. Sensible and latent heats of unconverted steam can be recovered effectively by a condenser working as a heat exchanger.

Faraday efficiency is can be given by eq.(2.10) as follows:

$$\varepsilon_f = \triangle G / (I \times E)$$
$$= 2.393 \times (E - \eta) \times Q / (I \times E)$$
$$= 2.393 \times 1.006[\mathrm{V}] \times 6.78[\mathrm{Ndm^3/h}] / 21.7[\mathrm{W}]$$
$$= 0.75$$

where 1.006 [V] is the IR-free voltage per cell derived from eq.(2.9) using steam conversion rate.

Using the L.H.V. at 25℃, $\triangle H_o$, energy efficiency is given by eq.(2.12) as follows:

$$\varepsilon_e = \triangle H_o / (I \times E)$$
$$= (241.84/3.6[\mathrm{W/mol}] \times 6.78[\mathrm{Ndm^3/h}] / 22.4[\mathrm{Ndm^3/mol}]) / 21.7[\mathrm{W}]$$
$$= 0.94$$

If we use the L.H.V. at temperature of 997℃ instead of $\triangle H_o$, －249.5kJ/mol, then ε_e is 0.97.

Dornier-system GmbH had integrated the HTES module assembled 10-cell electrolysis tubes on a support box made of an electrical insulation material of Alumina. The box was called a register and worked as a manifold to supply steam into the each tube and to collect produced hydrogen from the tubes. The electrolysis tubes were connected on the register by special joining techniques (not clear) to ensure gastightness against thermal expansion difference between the tube and the register. The Electrolysis tubes within the register were connected electrically in series. Ten modules had been assembled to a stack consisting of 1,000 cells, by which hydrogen could be produced at a maximum rate of 0.6 [$\mathrm{Nm^3/h}$] [15].

(2) United States

Westinghouse Electric. Co. had conducted the HTES test using the Westinghouse type tubular cell [16]. Typical test conditions and test results were as follows:

Electrolysis temperature	:	1000℃
Pressure	:	near atmospheric pressure
Inlet gas flow rate	:	183 Nml/min (H_2)／538 Nml/min (H_2O) (at standard conditions of 1atm and 0℃)
Active cell area	:	75 cm^2
Applied voltage	:	1.31 V
Applied current	:	30 A
Current density	:	0.4 A/cm^2
Applied power	:	30[A]x1.31[V] = 39.3 W
Electrical resistance	:	1.31[V]／30[A] = 0.044 Ω
Hydrogen content at outlet	:	66%
Steam conversion rate	:	54%
Hydrogen production rate	:	17.6 Ndm^3/h
Hydrogen production density	:	234 Nml/cm^2h
Hydrogen production rate per applied power	:	448 Nml/W (H_2)

Faraday efficiency is

$$\begin{aligned}\varepsilon_f &= \triangle G/(I\times E)\\ &= 2.393\times(E-\eta)\times Q/(I\times E)\\ &= 2.393\times 0.93[V]\times 17.6[Ndm^3/h]/39.3[W]\\ &= 0.997\end{aligned}$$

where 0.93 [V] is the IR-free voltage per cell derived from eq.(2.9) using steam conversion rate. Energy efficiency is

$$\begin{aligned}\varepsilon_e &= \triangle Ho/(I\times E)\\ &= (241.84/3.6\ [W/mol]\ \times\ 17.6[Ndm^3/h]/22.4[Ndm^3/mol])/39.3[W]\\ &= 1.34\end{aligned}$$

This energy efficiency shows very low ohmic loss in the cell. We, however, think that applied voltages presented in the paper might not be a proper terminal voltage between electrodes of the cell and/or a precise hydrogen content measured at outlet.

(3) Japan

Konishi et al. of the JAERI conducted the HTES tests using a tubular cell [1]. The cell had a simple structure coated platinum (Pt) paste for electrodes inside and outside a YSZ one-end-closed tube of 13mm in outer diameter and 9mm in inner diameter: the active cell area was 20cm^2. This type of electrolysis cell is for special use not but for commercial units. Then, they fabricated a electrolysis module which was one of components in a test apparatus of primary fuel cycle of a fusion reactor system installed at the Tritium Process Laboratory in the JAERI [17]. The electrolysis module consisted of 24 electrolysis tubes made of the YSZ tube coated Pt electrodes on the inner and outer tube surfaces. In the module specification, 6 mol/h of gas flow containing 0.18 mol/h of tritiated water steam could be processed. Hydrogen could be produced at a rate of 4 Ndm^3/h at 100% of steam conversion rate.

Recently, Hayashi et al. of the JAERI reported a HTES test results for decomposition of tritiated water steam [18]. They used a electrolysis module consisting of several self-supporting tubes with 5 cells which had almost the same configuration as that fabricated by Dornier -system GmbH. They produced hydrogen at a maximum rate of 25Ndm^3/h.

In JAERI, we are developing the HTES system for a hydrogen production plant aiming to connect to the HTGR. Our test results is described in the next chapter.

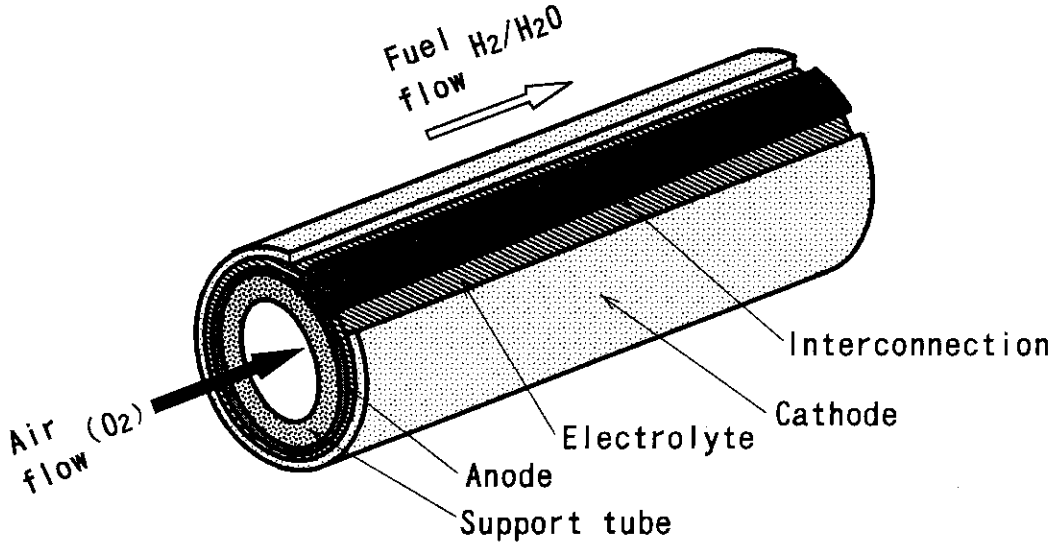

Fig.3.1 Single-cell tube (Westinghouse type)

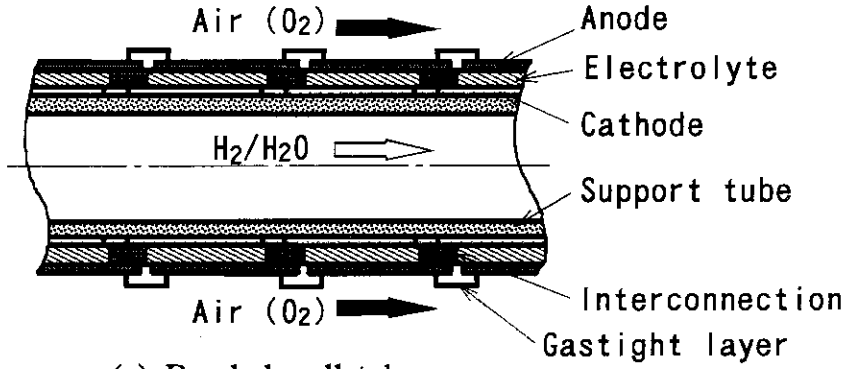

(a) Banded-cell tube

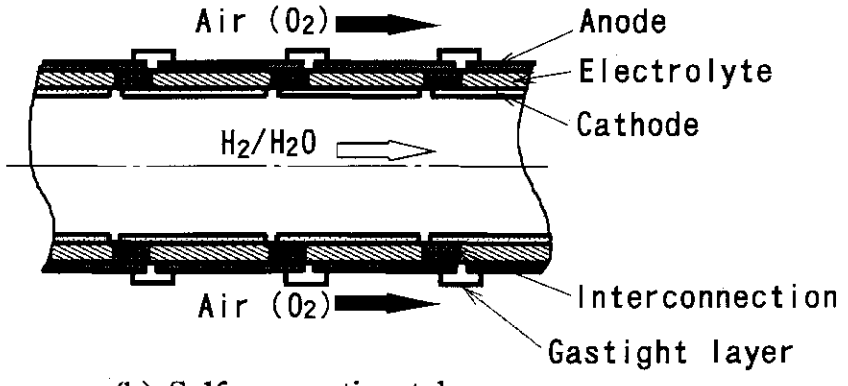

(b) Self-supporting tube

Fig.3.2 Multicell arrangement

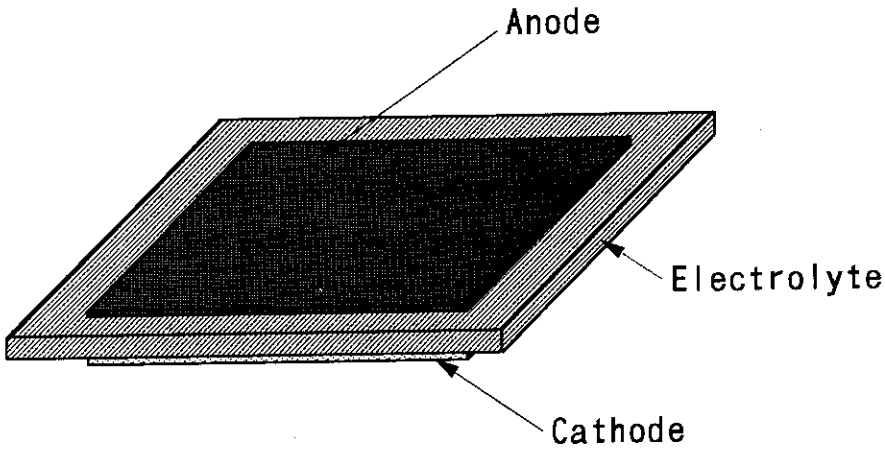

(a) Self-supporting cell

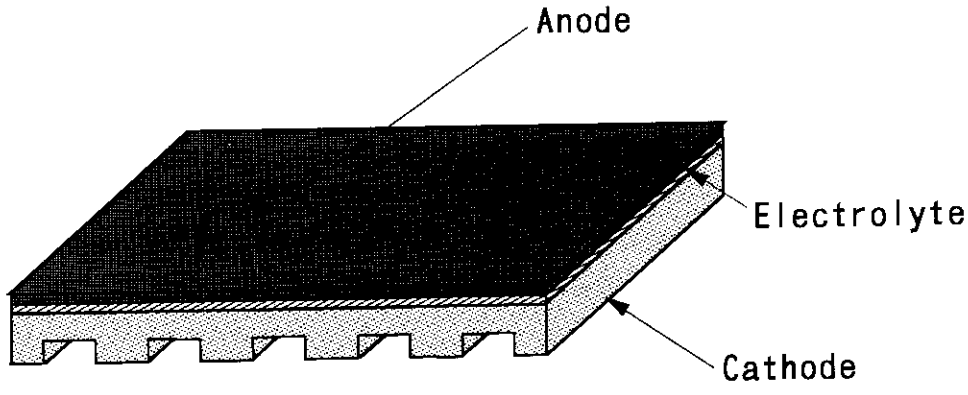

(b) Substrate-cell

Fig.3.3 Planar cell configuration

4. High-Temperature Electrolysis Tests with Tubular and Planar Cells

This chapter describes typical test results obtained by the electrolysis tube with 12 cells and preliminary test results obtained by the planar self-supporting cell conducted at Nuclear Heat Utilization Engineering Laboratory in the JAERI.

4.1 Test apparatus and test conditions for electrolysis tube

Figure 4.1 shows a structural drawing of the electrolysis tube of the banded-cell structure. The electrolysis tube was composed of 12 electrolysis cells of 19mm in length. These cells were connected in series electrically. Electrolyte of the cell was zirconia stabilized with 8 mol% yttria (YSZ) which is popular material in the SOFC as described before. The electrolyte layer was sandwiched between the porous cathode and anode layers: Ni cermet for the cathode and $LaCoO_3$ for the anode. At both ends of the electrolysis tube, platinum (Pt) wires for electric leads were welded on copper coating layers. Pt wires were connected with a DC power supply. The copper coating layers were connected with thin layers of electric conductors. Outside of the electrolysis tube was coated by thin gastight layers without the cells and the copper coatings. These layers were formed on a porous calcia-stabilized ZrO_2 (CSZ) tube (support tube or ceramic tube) of 22mm in outer diameter and 3mm in thickness by the plasma spraying. Thickness of each layers was in a range from 0.1mm to 0.25mm.

Figure 4.2 shows a schematic diagram of the test apparatus. Argon carrier gas from gas cylinders flowed into a humidifier at a constant flow rate and was mixed with steam at specific partial pressure through the humidifier where carrier gas bubbled through water controlled at a constant temperature. Mixed gas was supplied inside the electrolysis tube. Steam concentration was detected by dew point monitors both at the inlet and the outlet of the test section. Dry air from an air compressor was supplied outside the electrolysis tube at a constant flow rate in order not to decompose anode compound of $LaCoO_3$ under less oxygen partial pressure. Hydrogen concentration was measured by a gas chromatograph. Electrolysis voltage was applied by the DC power supply, and then, electrolysis current was measured through a standard resistor of 1 Ω.

Figure 4.3 shows a schematic drawing of the test section. The electrolysis tube was installed in a metallic tube (Inconel 600) of 50mm in inner diameter and was heated up to 1000℃ in a three-zone electric furnace. The electrolysis tube was fixed at the copper coatings with a metal tube by ground packing rings. Temperature of mixed gas,

steam/ argon carrier gas, was regulated to the test temperature by a sheath heater inserted in the electrolysis tube. Hydrogen produced inside the electrolysis tube (cathode side), unconverted steam and argon gas were cooled down to around 60℃ by a cooling pipe and then, were discharged to the atmosphere. High-temperature air mixed with oxygen produced in the anode side was cooled down to around 60℃ at the outlet of the metal tube and was also discharged to the atmosphere.

Tests were conducted under electrolysis temperatures of 850℃, 900℃, and 950℃. Other test conditions were as follows:

Argon flow rate : 2.2 Ndm^3/min
Dew point at the inlet of the electrolysis tube : 40℃～56℃
Steam content at the inlet of the electrolysis tube: 0.13～0.32 g/min
Air flow rate : 4～5 Ndm^3/min (dew point is less than -20℃)
Inlet pressure : 0.11 MPa (1.1 bar(abs))

In start-up and shut-down of the test section, increasing and decreasing rates of the furnace temperature were set at below 20℃/h in order not to generate large thermal expansion difference among the electrolysis tube components. Before applying electrolysis voltage, the cathode material, Ni cermet, was reduced with hydrogen mixed with argon carrier gas.

4.2 Test results obtained by electrolysis tube

Figure 4.4 shows a relationship between hydrogen production rate and applied power. Hydrogen production rate increased with the applied power and the electrolysis temperature. The maximum production rate was 3.9 Ndm^3/h at 15.7V, 1.42A and 850℃, 4.4 Ndm^3/h at 16.3V, 1.38A and 900℃, and 7.0 Ndm^3/h at 15.6V, 1.72A and 950℃, respectively. Then, hydrogen production density is 25 Nml/cm^2h at 850℃, 28 Nml/cm^2h at 900℃ and 44 Nml/cm2h at 950℃. Apparent electrical resistances including resistances of electrical leads and interconnections were around 11 Ω at 850℃ and 900℃, and around 9 Ω at 950℃. In the case of 950℃, Faraday efficiency was

$$\varepsilon_f = 2.393 \times 0.89[V] \times 7[Ndm^3/h] / (15.6[V] \times 1.72[A])$$
$$= 0.556$$

where 0.89V is the IR-free voltage derived from eq.(2.9) using steam conversion rate. This low Faraday efficiency was considered to be caused by following reasons:

- Ohmic loss was high at interconnections and electric lead layers,
- Concentration overvoltage increased, since steam could not supply enough to the cathode through support tube, and hydrogen produced at the cathode was not fully discharged into the main flow through the support tube.

In these tests, the steam conversion rate meaning an efficiency of steam utilization was less than 40%. The reason of low steam conversion rate was considered that steam could not permeate easily through the support tube to the cathode since the support tube had rather low porosity of around 38%. If steam reached to the cathode sufficiently, hydrogen production rate could increase more than the present results. The self-supporting cell structure, therefore, is considered to be better in the HTES than the banded-cell structure supported by the ceramic tube.

Figure 4.5 shows a relationship between applied power and combustion heat of produced hydrogen based on the standard enthalpy of formation, $\triangle H_o \times$ mole number of produced hydrogen. A quotient of (combustion heat of generated hydrogen/ applied power) is the energy efficiency. The energy efficiency increased with electrolysis temperature as shown in the figure. The energy efficiency in the case of 7 Ndm^3/h at 950℃ was, however, only about 80%. When high-temperature process heat and steam are supplied from the HTGR to a hydrogen production plant of the HTES, a plant operation temperature will be 900℃ at highest. From the view point, new better electrolytes working below 900℃ should be searched. One of candidates is ytterbia stabilized zirconia.

After the test, inspection found that large part of anode layers detached from the electrolyte layers, which served in one thermal cycle of increasing to electrolysis temperatures and then, decreasing down to the room temperature. Since the durability of the cell against thermal cycles is one of the key performance for the HTES, the plasma spraying technique should be improved so as to raise adhesion of the anode layer on the electrolyte layer against thermal expansion difference of these layers. Dornier-system GmbH, Westinghouse Co. and Konishi et al., however, have not reported the durability of the cell against thermal cycles.

4.3 Preliminary test results obtained by planar cell

On the basis of test results described above, we have tried to fabricate the self-supporting electrolysis tube. Its yield, however, was very low, and fabrication cost was

much higher than that of the banded-cell tube, because it was very difficult to manufacture electrolysis cylinders of 0.3mm thick and to connect segmented cells in series with gastight interconnections.

Then, we have focused on the planar cells, particularly self-supporting planar cell, from the viewpoint of mass production of the cell: quality control in the course of its production is much easier than the banded-cell tube, and its production technologies has been greatly progressed by the SOFC development. Present production cost of the self-supporting planar cell is 1/7 or less lower than that of the banded-cell tube shown in Fig. 4.1 and will be reduced further by mass production.

In progressing the HTES technology, especially the electrolysis cell technology, cooperation with cell-production companies is indispensable for the development of high-performance cells. So, we have started to cooperate with Fuji Electric Co. who is making good results in the planar type SOFC research field.

Figure 4.6 shows a structural drawing of the self-supporting planar cell made by Fuji Electric Co. The cell consists of the electrolyte plate of YSZ and porous electrodes. The YSZ plate is a 100mm square plate with thickness of 0.3mm, and electrodes are coated on the area of 80 x 80mm with thickness of less than 0.03mm. Material of the cathode is Ni cermet, and that of anode is strontium-doped $LaMnO_3$.

The cell is sandwiched with metal housings made of SUS-310S. Each housings have a metal rod for the electric lead, an inlet and an outlet pipings for gases, and Pt sheet of 0.1mm thick was welded on inner surface of each housings opposite to the electrodes of the cell. Metal rods and pipings are also made of SUS-310S. DC power supplies through the metal rods, housings, Pt sheets and wavy electrical lead plates to the cell. The wavy electrical lead plate made of Pt mesh was installed in each electrode compartment to work as the support of the cell against the pressure difference between electrodes as well as the electric lead. Compression seals were done at the edge of the cell plate: compression load was up to 20kg. Then, an alumina sheet of 0.3mm thick was inserted between the cell plate and the housing in the anode side to prevent from current leak through the cell plate edge.

The cell with housings was installed in a electric furnace and was heated to the test temperature. Steam was supplied to the cathode compartment with argon and hydrogen gases through a steam generator. Argon gas was the carrier gas of steam, and hydrogen a reduced gas to keep Ni of the cathode material from oxidation. Dry air was supplied to the anode compartment. Steam flow rate was controlled by water flow rate to the

steam generator, and flow rates of other gases were controlled by mass flow controllers. Hydrogen concentration was measured at the outlet of the cathode compartment by the gas chromatograph. Electrolysis voltage was applied by the DC power supply.

A preliminary test was conducted under following conditions:

Electrolysis temperature	:	850℃
Inlet gas flow rate	:	0.2 Ndm^3/min (argon gas)
		0.1 Ndm^3/min (H_2)
Steam flow rate	:	0.3 g/min
Air flow rate	:	1 Ndm^3/min
		(dew point is less than -20℃)
Inlet pressure	:	～0.14 MPa (～1.4 bar(abs))

Figure 4.7 shows a relationship between hydrogen production rate and applied power. Maximum hydrogen production rate was 2.3 Ndm^3/h at the applied power of 10.8W: applied voltage and current were 2.8V and 3.87A, and then, the apparent electrical resistance was 0.7 Ω. Hydrogen production density is 36 Nml/cm^2h and is about 1.4 times higher than that obtained by the electrolysis tube at 850℃. Then, Faraday efficiency was

$$\varepsilon_f = 2.393 \times 0.88[V] \times 2.3[Ndm^3/h] / (3.87[A] \times 2.8[V])$$
$$= 0.45$$

where 0.88V is the IR-free voltage derived from eq.(2.9) using steam conversion rate. This low Faraday efficiency was considered to be caused by nonuniform current density on the electrodes because electrical lead plates could not contact well with electrode surfaces.

Figure 4.8 shows a relationship between applied power and combustion heat of produced hydrogen based on the L.H.V. at 25℃, $\triangle H_o \times$mole number of produced hydrogen. A quotient of (combustion heat of generated hydrogen/ applied power) is the energy efficiency. The energy efficiency at 2.3 Ndm^3/h of hydrogen production rate was around 0.7, and was higher than that obtained at 850℃ by the electrolysis tube shown in the **Fig. 4.5**. Since this test results were obtained in the first preliminary test, we can only say the test results qualitatively. We are now improving the test apparatus and a measurement system to obtain precise data.

In addition, gas leakage from the cell plate edges was less than 10%. Further

development of high-temperature seals is needed for the high-pressure operation up to 4MPa. After the test, we found that a part of the cell plate edge was cracked. This would be caused by a thermal expansion difference between the cell and housings under the compression seal.

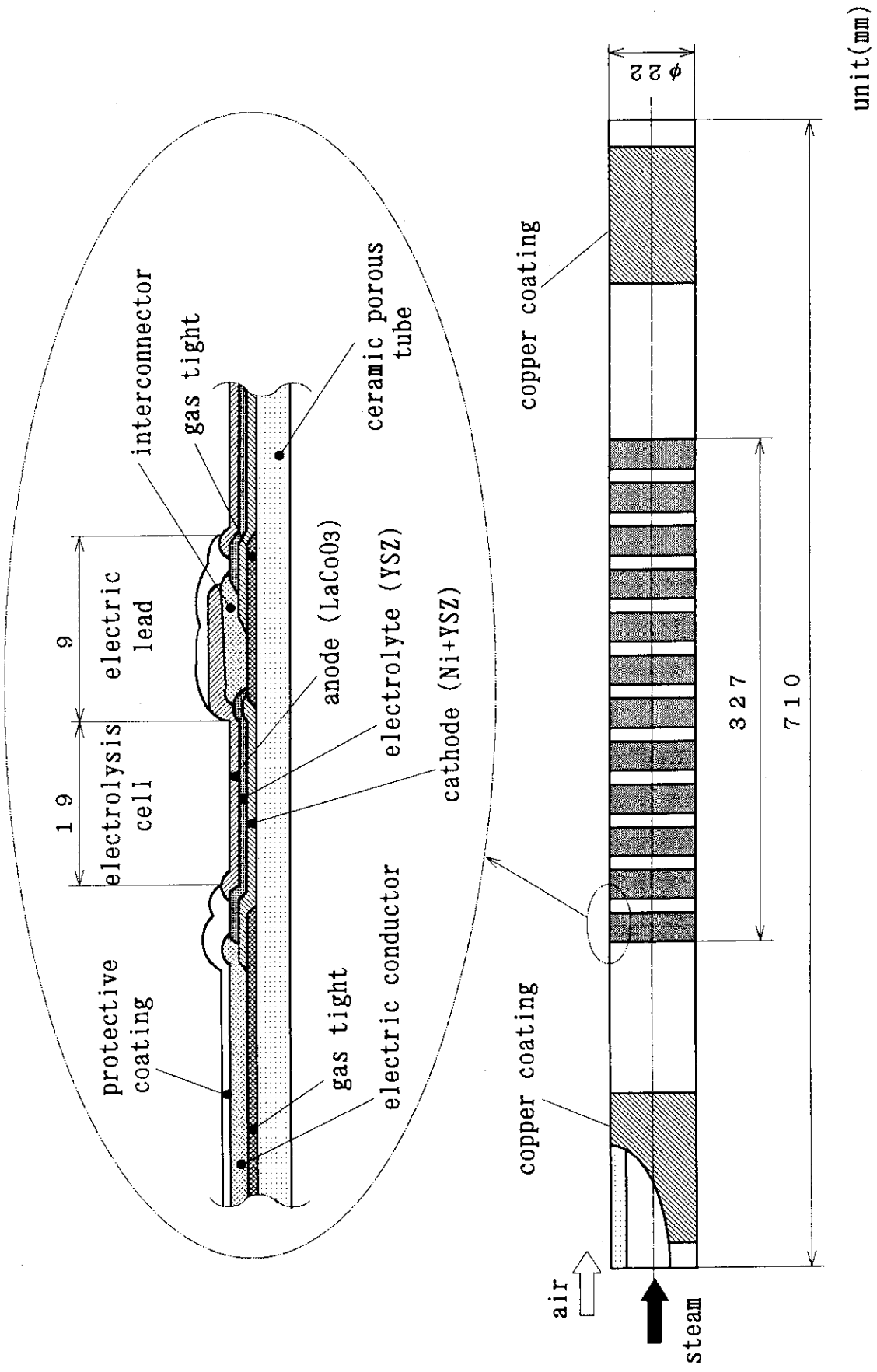

Fig. 4.1 Structural drawing of electrolysis tube with 12 cells

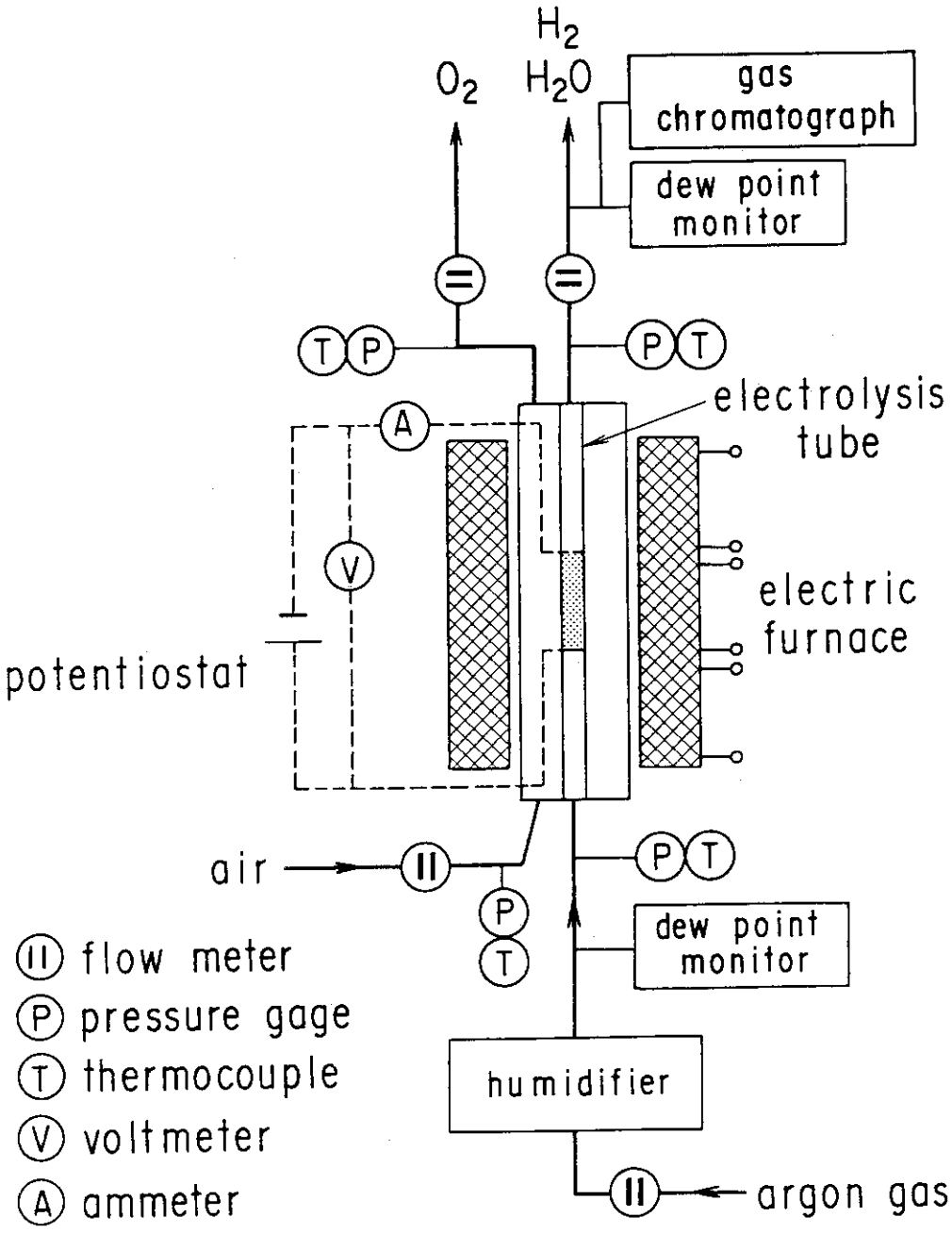

Fig. 4.2 Schematic diagram of test apparatus

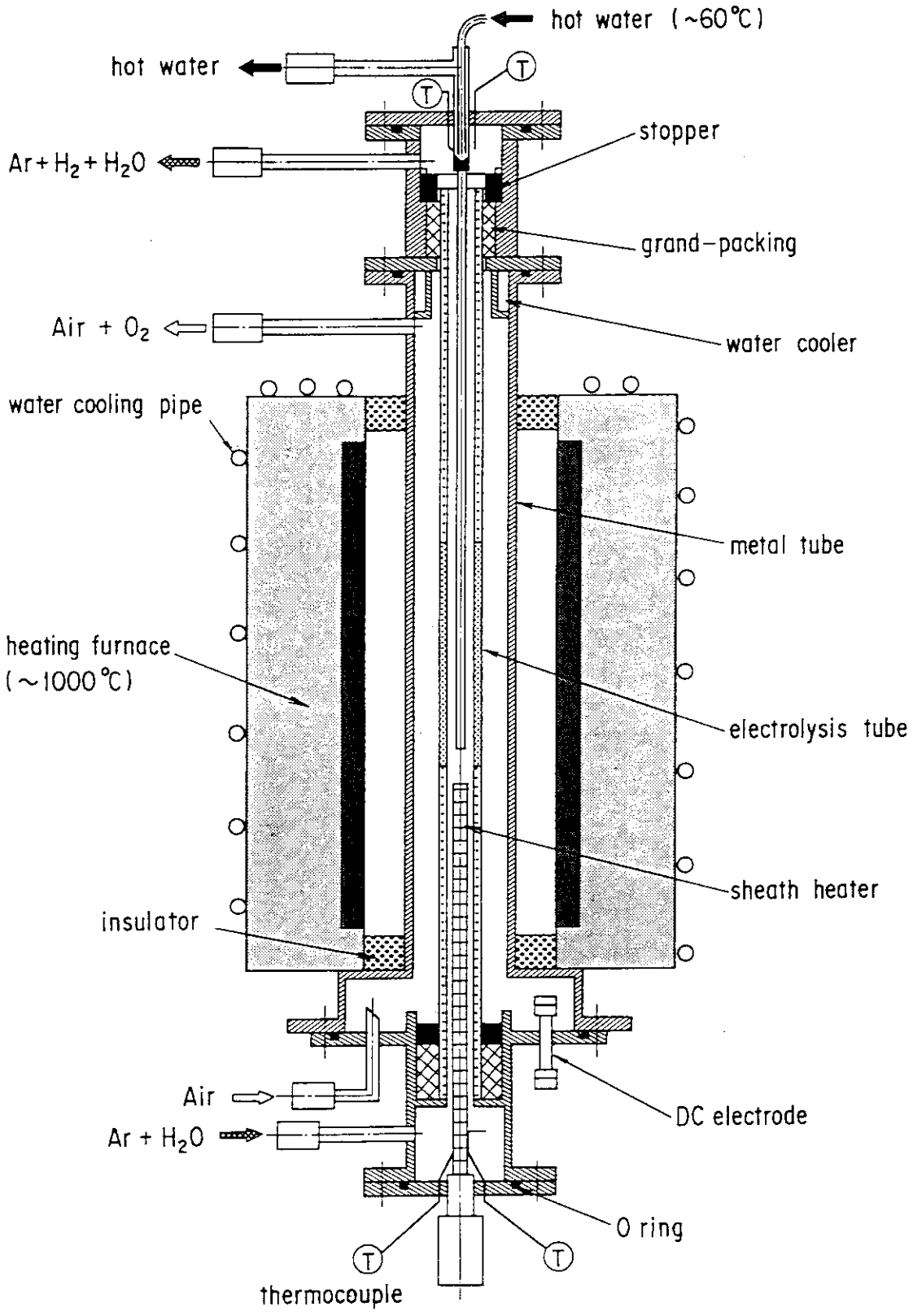

Fig. 4.3 Schematic drawing of test section with electrolysis tube

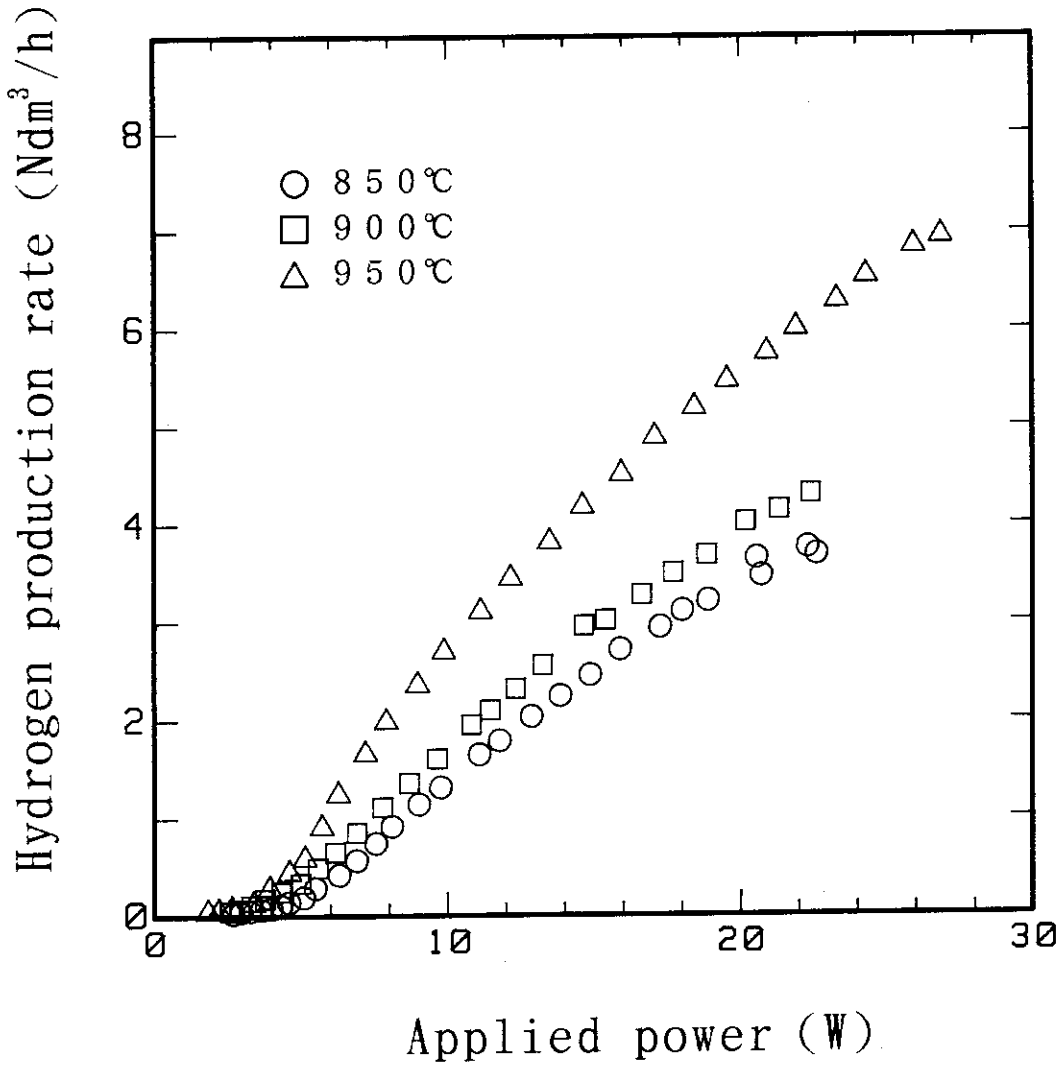

Fig. 4.4 Relationship between hydrogen production rate and applied power obtained by electrolysis tube

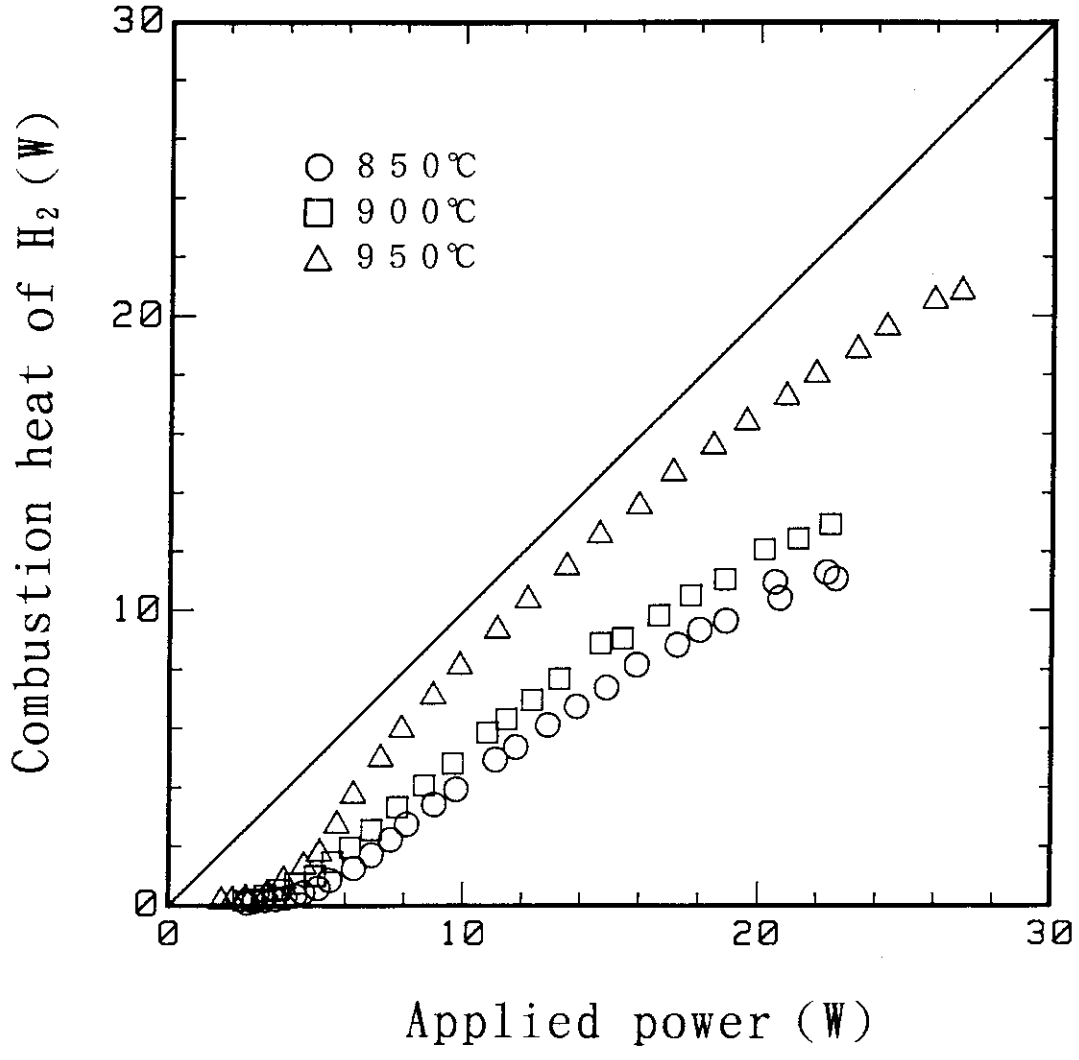

Fig. 4.5 Relationship between applied power and combustion heat of generated hydrogen obtained by electrolysis tube

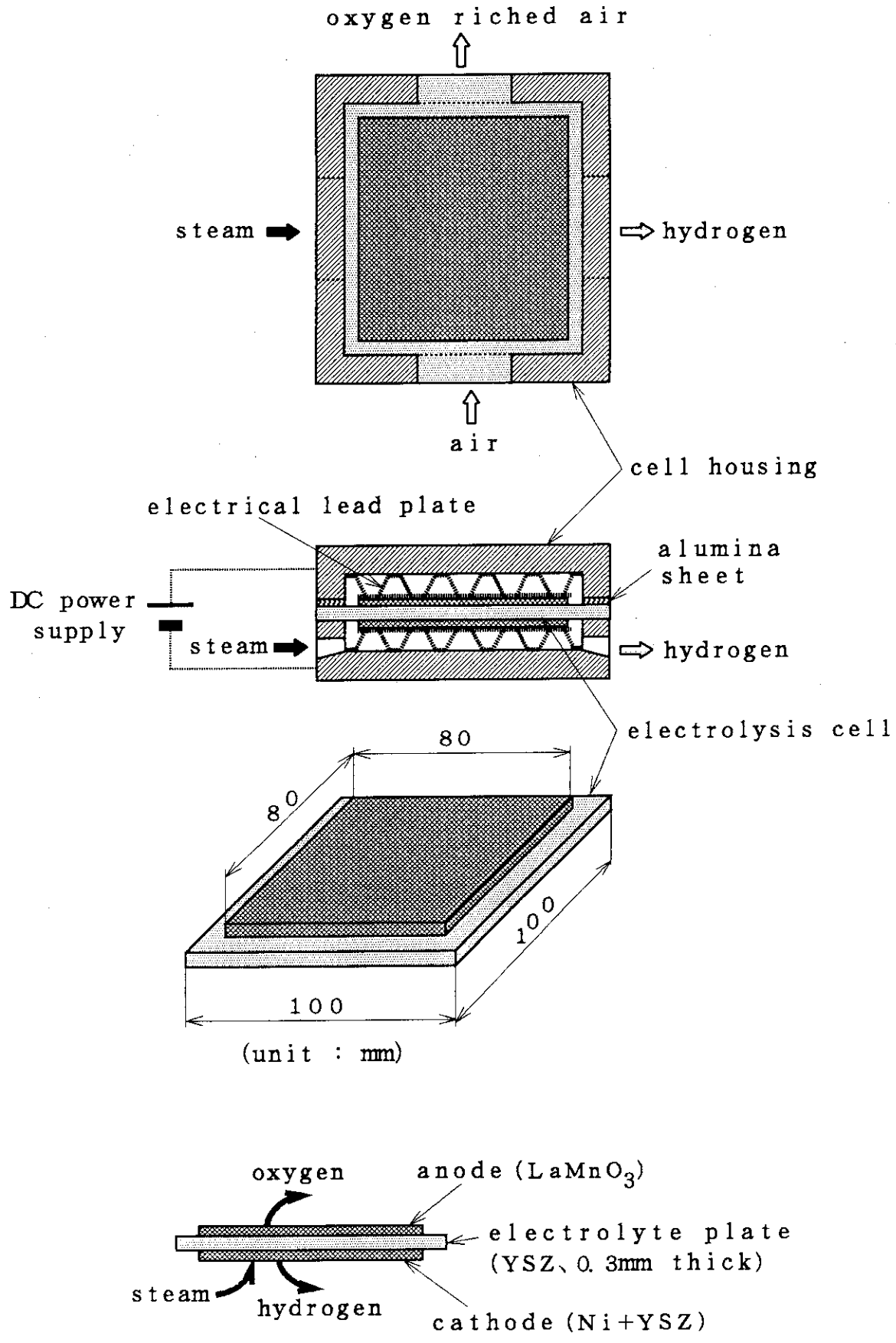

Fig. 4.6 Structural drawing of self-supporting planar cell

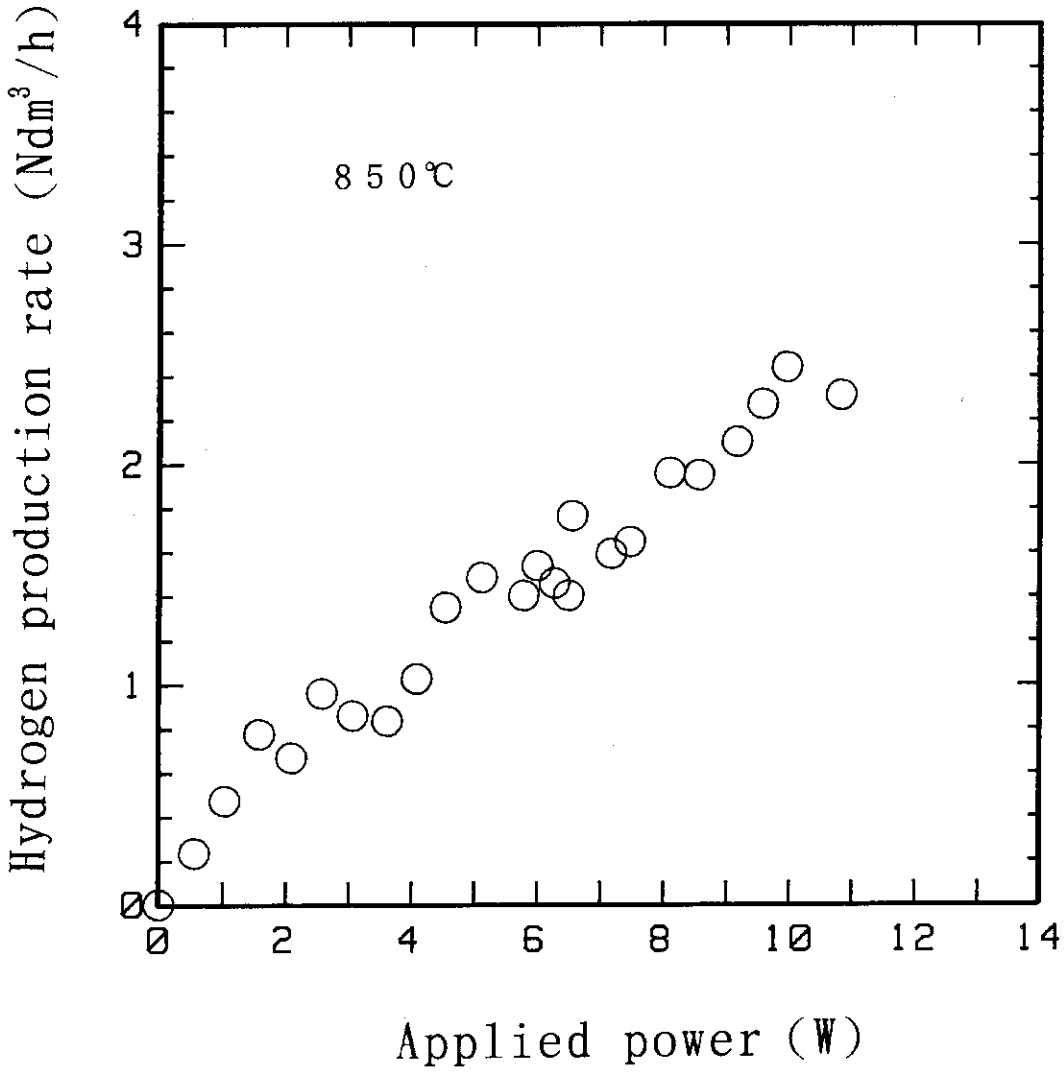

Fig. 4.7 Relationship between hydrogen production rate and applied power obtained by planar cell

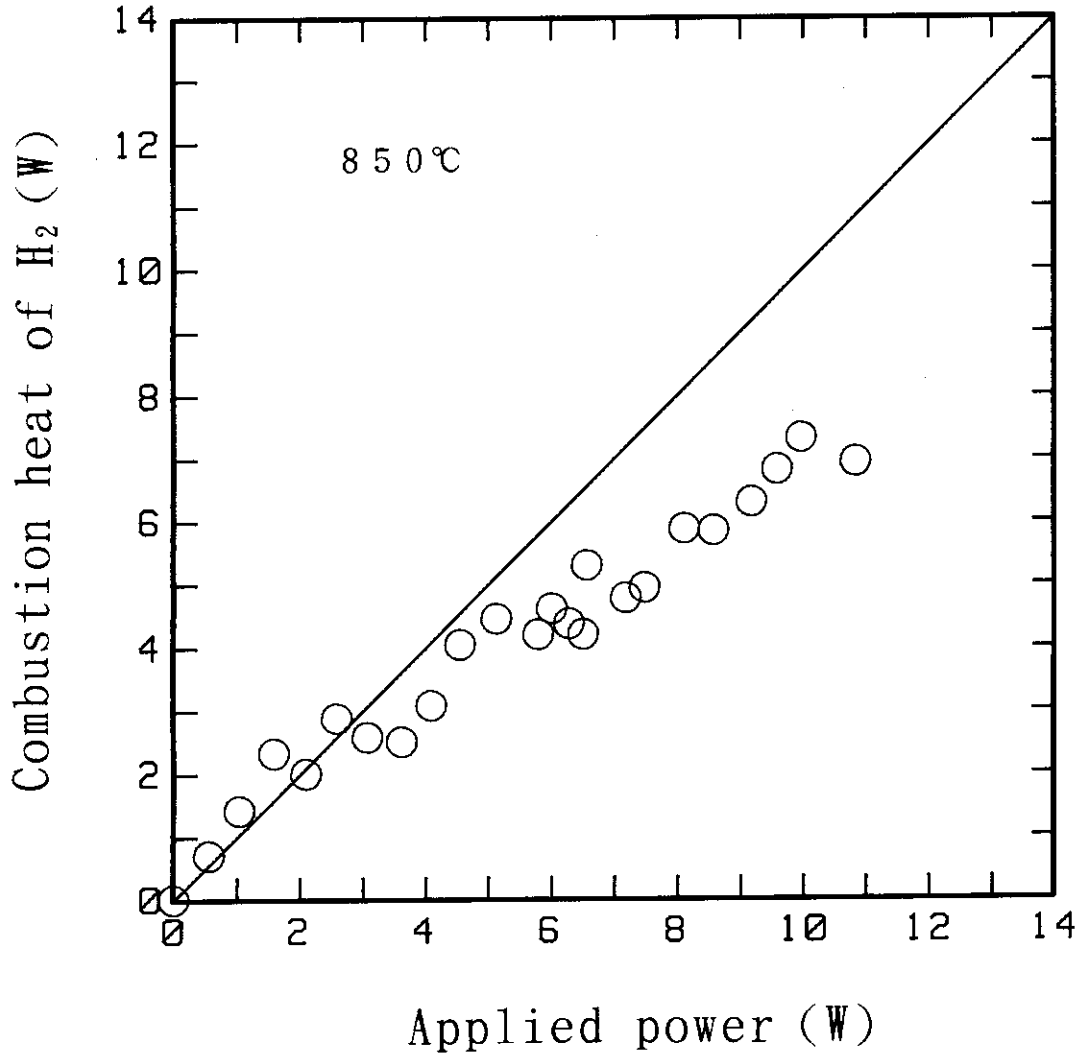

Fig. 4.8 Relationship between applied power and combustion heat of generated hydrogen obtained by planar cell

5. Future Works

Many severe problems common to all high-temperature designs and operations are inherent in the HTES technology. This chapter presents the outline of technological issues to improve electrolysis cells and to fabricate the electrolysis module. In addition, it describes the thinking way of optimization of the HTES system and the demonstration test plan using large-scale modules (electrolysis units) for finally connecting to the HTTR as a nuclear process heat utilization system.

5.1 Improvement of electrolysis cell

The HTES is an innovative concept at an early stage of electrolysis technology. It has been only shown a feasibility to produce hydrogen continuously by the HTES as described in the former chapters. The HTES technology progress requires continuous efforts to improve existing electrolysis cells to suitable cells for the HTES. Improvements of electrolysis cells are:

- to reduce ohmic loss of the cell to raise the energy efficiency, and
- to increase the cell durability against heat cycles for demonstration units.

If it is possible to operate the cell at low temperature below 900℃ with high energy efficiency by reducing ohmic loss of the cell, the HTES system will be suitable for the nuclear process heat application.

(1) Cell materials

The characteristics of cell materials required for minimum ohmic loss of the cell are as follows:

- Electrolyte of minimal thickness with gastightness and suitable ionic conductivity: Ytterbia stabilized zirconia has higher ionic conductivity than that of YSZ, but is more expensive than YSZ.
- Electrodes with much higher electron conductivity than that of presently used materials such as $LaCoO_3$ or $LaMnO_3$ for the anode and Ni cermet for the cathode;
  - They should be stable against the respective oxidation and reduction reactions in the hydrogen/steam and oxygen environments and must permit ready diffusion of gases and steam;
  - The interconnection, the electric lead layer, and the electric plate are required for the same performance as that of the electrode;

- Those materials are to be inexpensive.

As for the self-supporting planar cell, the ohmic loss of electric paths excluding the cell can decrease with contact electrical resistance of the electrical lead plates against the cell electrodes and others. So, the electrical lead plate requires large contact area with electric surfaces of the housings and electrodes of the cell as well as its own low electrical resistance.

Furthermore, we have to develop inexpensive and high-performance sealant materials without leakage of hydrogen under high-temperature and high-pressure conditions and with resistance to steam corrosion and air oxidization: the sealant material, then, should function as an electrical insulator and an absorber of thermal expansion in order to keep from electrical shorting and to improve the cell durability.

In parallel to above technological improvements, we should take efforts to elucidate electrochemical reaction mechanisms and kinetics on and around electrode surfaces and to investigate effects of heat and mass transfer rates around electrodes and in the electrolyte on overvoltages and ohmic losses.

(2) Cell strength and durability against heat cycles

Selecting cell materials, we should take into consideration maintaining cell mechanical strength, and increasing durability of the cell against heat cycles. On mechanical strength of the cell, supporting structure cells such as the single-cell tube, the banded-cell tube or the substrate-supporting planar cell described in chapter 3 are much better than the self-supporting cell.

The self-supporting planar cell is, however, possible to keep the cell mechanical strength by the electrical lead plates and interconnections mentioned in the next section. These components work as a support of the cell as well as the electric lead. The electrical lead plates must be designed:

- to provide large contact area with electric surfaces such as electrodes in order to achieve uniform current density on the electrode;
- to keep high electron conductivity under high-temperature condition; and
- not to prevent permeation of gases and steam to the electrode.

On the other hand, adhesion of electrodes' layers to the electrolyte is the key parameter of the cell durability against heat cycles. CVD, EVD or the plasma spraying are better techniques to make electrode layers with high adhesion, but are not for mass

production because of their high cost and rather low yield. The slurry coating applied in fabricating the self-supporting planar cells mentioned in former chapters, however, is the lowest-cost and higher-yield technique, which are suitable for mass production. In addition, it is possible to improve adhesion of electrodes' layers by changing sintering temperature up to 1300℃ after coating electrode slurries on the electrolyte. We have to improve electrode coating techniques further to increase adhesion and yield, and to lower the coating cost for mass production.

In parallel to improve the cell strength and the cell durability, we have to take efforts to scale-up cell sizes for electrolysis units: long electrolysis tubes with large diameter and large planar cells with rectangular or circular shape. Since yield of the cell usually lower with enlarging cell size, fabrication techniques - mainly coating techniques - have to be improved further.

5.2 Bench-scale test by electrolysis module

In the course of improving the electrolysis cell, we will be able to fabricate lower-cost electrolysis tubes or planar cells with higher electrolysis performance. Then, we will design and fabricate the electrolysis module containing several electrolysis tubes or planar cells. In designing the module, we have to make better contrivance of following parts:

- Electrical connections working under a high-temperature condition.
- Manifold distributing steam to each cell uniformly.
- Seal configuration working without leakage of steam/hydrogen and air under high-pressure operation; and with a function absorbing thermal expansion in the module.

In addition, we have to design the special parts of the interconnection with appropriate configurations to achieve uniform steam concentration on the cathode surface in stacking planar cell for the module. **Figure 5.1** shows a concept of planar cell module. In this module, the interconnection is inserted between the cells to separate steam/hydrogen and air paths as well as to keep electric path as electric collectors. Thus, the interconnection is required for combined characteristics of low gas permeability, low ohmic resistance, high mechanical strength, long life in a oxidation and reduction environment, and durability against heat cycles, to say noting of inexpensive. We consider that it will be better to insert the wavy electrical lead plate made of a meshed noble metal between the interconnection and the cell as a buffer against thermal stresses.

After designing, we will fabricate the small-sized module containing several electrolysis tubes or planar cells and will investigate following items to obtain design data for demonstration units with hydrogen production of 10 Nm^3/h mentioned in the next section.

- Long-term stability of module operation: for more than 5000h at a temperature of 700 to 900℃ and pressure up to 1MPa.
- Hydrogen production efficiency (energy efficiency).
- An amount of leakage of hydrogen from the seals.
- Applied power distribution and cell ohmic losses.
- Concentration distributions of steam/hydrogen.
- Flow rate distribution and pressure loss.
- Pressure difference controlability: below 4.9KPa (500mmH_2O).
- Applied power controlability against change of steam flow rate.
- Durability against heat cycles.

5.3 System optimization

System optimization calls for an analysis of an integrated system consisting of the electrolysis units and all the ancillary equipment such as steam generators, steam super heaters, and heat exchangers. Then, high-temperature heat will supply from the HTGR through a intermediate heat exchanger. The integrated system of the HTES using nuclear process heat will be more complicated than that for the conventional water electrolysis

In developing an analysis code, the code should provide functions to be capable of accounting for the effects of all major operating variables such as flow rate, pressure and temperature on the hydrogen production efficiency; and for the effects of the emergency shut-down of the HTGR on the HTES system. From the analysis, we will be able to determine the optimum flowsheet of a demonstration system connected to the HENDEL mentioned in the next section and capacities of installing equipments.

In making the system flowsheet, heat exchangers to recover heat content of the product gases with the feed steam should be installed at the outlet of the electrolysis units in order to reduce the net energy input required. The feed steam could then be heated to cell operating temperature by a high-temperature heat from the Helium Engineering Demonstration Loop (HENDEL) of the JAERI.

In addition, small amount of hydrogen should be supplied to the electrolysis units to prevent oxidation of the electrolysis cell cathodes. This requirement leads to the inclusion of a hydrogen recycle stream in the flowsheet. Use of oxidation-resistant cathodes such as platinum could eliminate the hydrogen recycle stream.

Through the analysis, we should also determine procedures coping with the abnormal states as follows:

- decreasing steam and air flow rate rapidly,
- increasing pressure difference between anode and cathode compartments.

When steam flow rate decreases rapidly, applied power to electrolysis units should be decreased immediately to prevent increasing cell temperature by Joule heating. Lack of steam at the cathode makes the overvolatge increase. Delicate control of pressure difference between anode and cathode compartments is indispensable for preventing failure of electrolysis cells under high-pressure operation.

In parallel to analysis, following ancillary equipments and systems have to be developed:

- The steam super heater which can heat steam up to 900℃,
- The heat exchanger recovering heat content of the product gases with the feed steam,
- Control system of pressure difference between anode and cathode compartments, which consists of high-speed valves, pressure dampers and so forth.

5.4 Outline of demonstration tests

We have a plan to perform demonstration tests of the HTES with the HENDEL for connecting to the HTTR. The flowsheets for demonstration tests will be determined by the above analysis. Simulated process heat of high-temperature and high-pressure helium gas of up to 950℃ and 4MPa will be supplied from the HENDEL.

Demonstration tests will be performed at two stages. The first stage is an engineering demonstration of the HTES system using electrolysis units of which hydrogen production rate will be 10Nm^3/h. Using this system,

- the analysis results of the system mentioned above will be verified,
- long-term stability and durability of the electrolysis units will be demonstrated, and

- operational procedures will be established: the start-up, the shut-down, and the emergency operation at the abnormal states such as decrease of steam flow rate and temperature, and increase of pressure difference on the cells.

On the basis of the test results obtained by above demonstration test, the system will be rearranged and be enlarged to a prototype system of 100Nm^3/h of hydrogen production rate as a second stage. Tests in the second stage will be performed to obtain demonstration data for safety review of the HTTR heat utilization system.

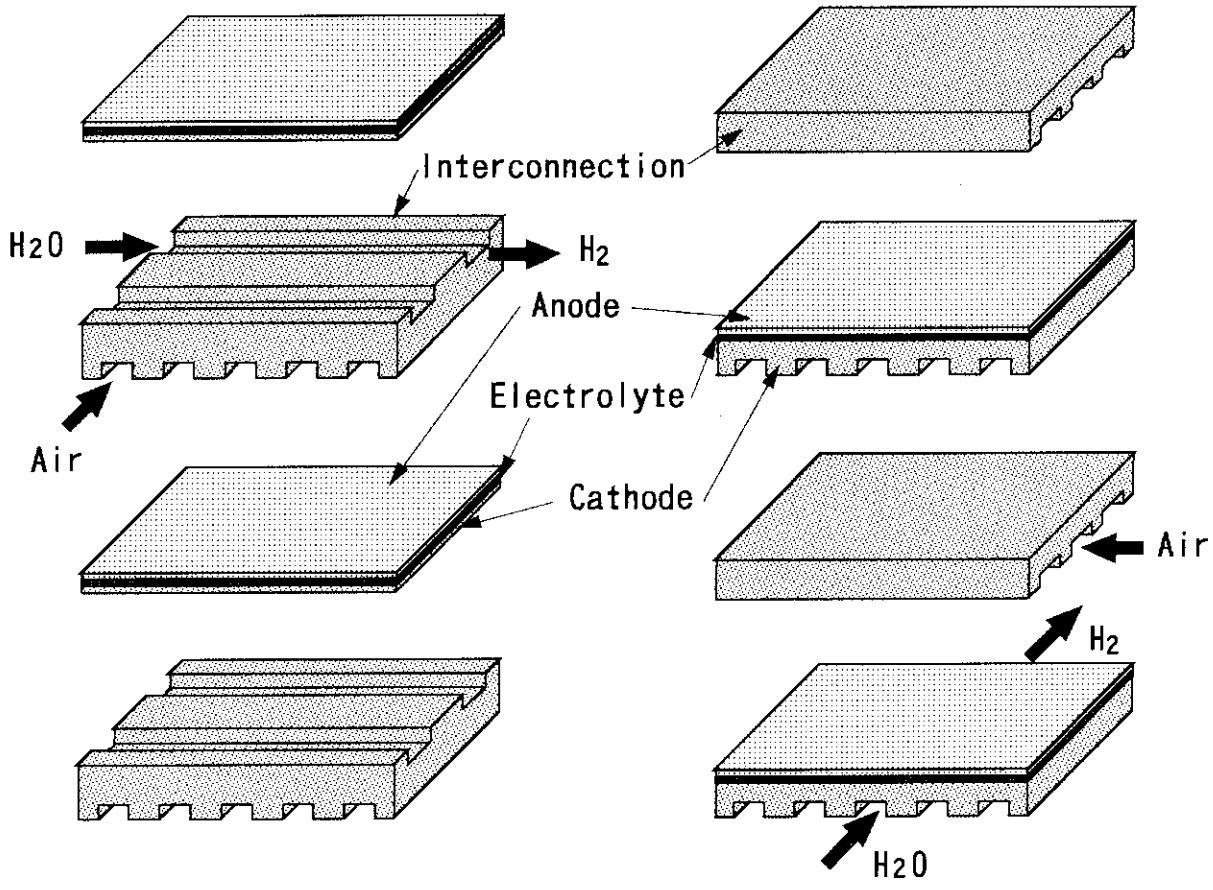

(a) Self-supporting structure　　(b) Substrate structure

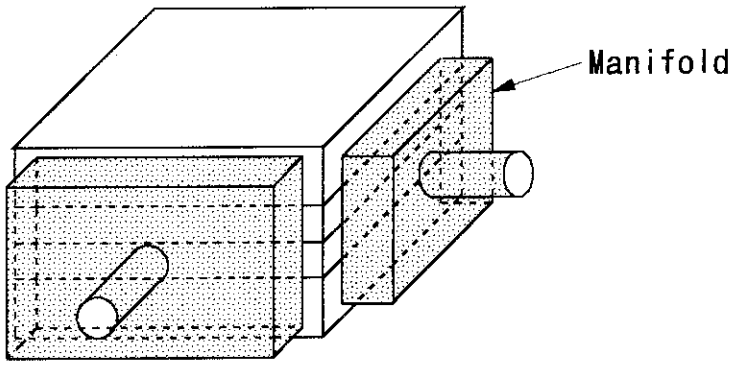

(c) Cell stack

Fig.5.1 Schematic drawing of planar cell module

Acknowledgments

We will express our gratitude to Dr. T. Yasuno and Dr. N. Wakayama of the former head of Department of High Temperature Engineering, JAERI, Dr. T. Nakanishi, Mr. F. Okamoto, and Mr. Y. Yamada of Fuji Electric Co. for supporting our HTES tests. We will thanks to Mr. S. Shimizu of High Temperature Engineering and Dr. K. Hada of Department of HTTR Project, JAERI, for useful discussions on contents of the this report.

References

[1] S. Konishi et al., "Solid Oxide Electrolysis Cell for Decomposition of Tritiated Water", Int. J. Hydrogen Energy, 11, 507-512(1986).

[2] B. C. H. Steele, "Properties and Performance of Materials Incorporated in SOFC Systems", Proc. International Symp. on SOFC, Nagoya, 136-147(1989).

[3] N. Q. Minh, "Ceramic Fuel cells", J. Am. Soc., 76, 563-588(1993).

[4] A. Kusunoki et al. "A 25kW SOFC Generation System Verification Test SOFC (written in Japanese)", Extended abst. of 2nd Symp. SOFC in Japan, 19-22(1993).

[5] F. Umemura et al., "Development of Solid Oxide Fuel Cell", Proc. International Symp. on SOFC, Nagoya, 25-32(1989).

[6] N. Murakami et al., "Development of Solid Oxide Fuel Cells (written in Japanese)", MHI Technical Report, 29, 182-187(1992).

[7] T. Okuo et al., "Studies on SOFC Components for Low Temperature Operation System - Development of Metallic Porous Tube and Its Application (written in Japanese)", Extended abst. of 2nd Symp. SOFC in Japan, 49-56(1993).

[8] W. Doenitz et al., "Electrochemical High Temperature Technology for Hydrogen Production or Direct Electricity Generation", Int. J. Hydrogen Energy, 13, 283-287(1988).

[9] W. Doenitz et al., "Concepts and Design for Scaling Up High-Temperature Water Vapor Electrolysis", Int. J. Hydrogen Energy, 7, 321-330(1982).

[10] H. Itoh et al., "Development of Solid Oxide Fuel Cells - Producing Cost Estimation (written in Japanese)", Central Research Institute of Electric Power Industry, Yokosuka Research Laboratory Report, No.W92028(1993).

[11] T. Nakanishi et al., "Planar Solid Oxide Fuel Cell Technology preliminary Cell Performance and Stack Configuration", Proc. International Symp. on SOFC, Nagoya, 43-49(1989).

Acknowledgments

We will express our gratitude to Dr. T. Yasuno and Dr. N. Wakayama of the former head of Department of High Temperature Engineering, JAERI, Dr. T. Nakanishi, Mr. F. Okamoto, and Mr. Y. Yamada of Fuji Electric Co. for supporting our HTES tests. We will thanks to Mr. S. Shimizu of High Temperature Engineering and Dr. K. Hada of Department of HTTR Project, JAERI, for useful discussions on contents of the this report.

References

[1] S. Konishi et al., "Solid Oxide Electrolysis Cell for Decomposition of Tritiated Water", Int. J. Hydrogen Energy, 11, 507-512(1986).

[2] B. C. H. Steele, "Properties and Performance of Materials Incorporated in SOFC Systems", Proc. International Symp. on SOFC, Nagoya, 136-147(1989).

[3] N. Q. Minh, "Ceramic Fuel cells", J. Am. Soc., 76, 563-588(1993).

[4] A. Kusunoki et al. "A 25kW SOFC Generation System Verification Test SOFC (written in Japanese)", Extended abst. of 2nd Symp. SOFC in Japan, 19-22(1993).

[5] F. Umemura et al., "Development of Solid Oxide Fuel Cell", Proc. International Symp. on SOFC, Nagoya, 25-32(1989).

[6] N. Murakami et al., "Development of Solid Oxide Fuel Cells (written in Japanese)", MHI Technical Report, 29, 182-187(1992).

[7] T. Okuo et al., "Studies on SOFC Components for Low Temperature Operation System - Development of Metallic Porous Tube and Its Application (written in Japanese)", Extended abst. of 2nd Symp. SOFC in Japan, 49-56(1993).

[8] W. Doenitz et al., "Electrochemical High Temperature Technology for Hydrogen Production or Direct Electricity Generation", Int. J. Hydrogen Energy, 13, 283-287(1988).

[9] W. Doenitz et al., "Concepts and Design for Scaling Up High-Temperature Water Vapor Electrolysis", Int. J. Hydrogen Energy, 7, 321-330(1982).

[10] H. Itoh et al., "Development of Solid Oxide Fuel Cells - Producing Cost Estimation (written in Japanese)", Central Research Institute of Electric Power Industry, Yokosuka Research Laboratory Report, No.W92028(1993).

[11] T. Nakanishi et al., "Planar Solid Oxide Fuel Cell Technology preliminary Cell Performance and Stack Configuration", Proc. International Symp. on SOFC, Nagoya, 43-49(1989).

[12] T. Iwata et al., "Development of Substrata Type Planar SOFC at Fuji Electric (written in Japanese)", Extended abst. of 2nd Symp. SOFC in Japan, 1-4(1993).

[13] W. Doenitz et al., "High-temperature Electrolysis of Water Vapor Status of Development and Perspective for Application", Int. J. Hydrogen Energy, 10, 291-295(1985).

[14] F. J. Salzano et al., "Water Vapor Electrolysis at High Temperature: Systems Consideration and Benefits", Int. J. Hydrogen Energy, 10, 801-809(1985).

[15] W. Doenitz et al., "Recent Advances in the Development of High-temperature Electrolysis Technology in Germany", 7th World Hydrogen Energy Conf., Moscow, Sept. (1988).

[16] N. J. Maskalick, "High Temperature Electrolysis Cell Performance Characterization", Int. J. Hydrogen Energy, , 563-570(1986).

[17] S. Konishi et al., "Experimental Apparatus for the Fuel Cleanup Process in the Tritium Process Laboratory", Fusion Technology, 14, 596-601(1988).

[18] T. Hayashi et al., "Joint operation of the TSTA under the Collaboration between JAERI and U.S.-DOE - TSTA extended loop operation with 100 grams of tritium on Apr.-May 1992 " , JAERI-M 93-083 (1993).